

From spectra to plant functional traits: Transferable multi-trait models from heterogeneous and sparse data

Eya Cherif^{a,b,*}, Hannes Feilhauer^{a,b,c,d}, Katja Berger^{e,f}, Phuong D. Daoⁱ, Michael Ewald^g, Tobias B. Hank^h, Yuhong He^j, Kyle R. Kovachⁱ, Bing Lu^k, Philip A. Townsendⁱ, Teja Kattenborn^{a,c}

^a Remote Sensing Centre for Earth System Research (RSC4Earth), Leipzig University, Talstr. 35, 04103 Leipzig, Germany

^b Center for scalable data analytics and artificial intelligence (ScaDS.AI), Leipzig University, Humboldtstr. 25, 04105 Leipzig, Germany

^c German Centre for Integrative Biodiversity Research (iDiv), Halle-Jena-Leipzig, Germany

^d Helmholtz-Centre for Environmental Research (UFZ), Leipzig, Germany

^e Image Processing Laboratory (IPL), Parc Científic, Universitat de València, València, Spain

^f Mantle Labs GmbH, Vienna, Austria

^g Institute of Geography and Geoecology, Karlsruhe Institute of Technology (KIT), Kaiserstr. 12, 76131 Karlsruhe, Germany

^h Department of Geography, Faculty of Geosciences, Ludwig-Maximilians-Universität München (LMU), Luisenstr. 37, 80333 Munich, Germany

ⁱ Department of Forest and Wildlife Ecology, University of Wisconsin-Madison, 1630 Linden Drive, Madison, WI 53706, USA

^j Department of Geography, Geomatics and Environment, University of Toronto, 3359 Mississauga Road, Mississauga, ON L5L 1C6, Canada

^k Department of Geography, Simon Fraser University, 8888 University Drive, Burnaby, BC V5A 1S6, Canada

ARTICLE INFO

Edited by Jing M. Chen

Keywords:

Hyperspectral remote sensing
Plant trait retrieval
Deep learning
Biophysical variables
Imaging spectroscopy
Canopy properties
Weakly supervised learning
Multi-task regression

ABSTRACT

Large-scale information on several vegetation properties ('plant traits') is critical to assess ecosystem functioning, functional diversity and their role in the Earth system. Hyperspectral remote sensing of plant canopies offers a key tool to map multiple plant traits. However, we are still lacking generalized methods to translate hyperspectral reflectance into a suite of relevant plant traits across biomes, land cover and sensor types. The absence of globally representative data sets and the gap between the available reflectance data with corresponding in-situ measurements have hampered such approaches. In recent years, the scientific community acquired multiple data sets encompassing canopy hyperspectral reflectance and plant traits from different plant types and sensors. To combine these heterogeneous data sets, we propose three multi-trait modeling approaches based on Convolutional Neural Networks (CNNs) to simultaneously infer a broad set of 20 structural and chemical traits (e.g. leaf mass per area, leaf area index, pigments, nitrogen). The performance of these multi-trait CNN models predicting these traits was compared against single-trait CNN as well as single-trait partial least squares regression (PLSR). We found that the multi-trait CNNs performances significantly increased from single-trait CNNs (nRMSE = 0.027–19.61%) and the state-of-the-art PLSR models (nRMSE = 1.94–40.07%) across a broad range of vegetation types (crops, forest, tundra, grassland, shrubland) and sensor types. Thus, providing a single model for multiple traits not only proved to be computationally more efficient, but also more accurate, since it enabled the model to incorporate traits' co-variation. Despite the data heterogeneity of the merged data set, our models performances' were comparable or exceeded those of previous studies. Overall, this study highlights the potential of weakly supervised approaches to overcome the scarcity of in-situ measurements and take a step forward in creating efficient predictive models of multiple biochemical and biophysical vegetation properties.

1. Introduction

Plant functional traits are key for assessing and monitoring terrestrial ecosystem properties. They provide insights on functional diversity and

can enhance our understanding of ecosystem functioning (Lavorel and Garnier, 2002; Migliavacca et al., 2021). Traits determine plant productivity and stress resistance and thus also how plants compete for growth and survival in different environments (Funk et al., 2017). For

* Corresponding author at: Remote Sensing Centre for Earth System Research (RSC4Earth), Leipzig University, Talstr. 35, 04103 Leipzig, Germany.
E-mail address: eya.cherif@informatik.uni-leipzig.de (E. Cherif).

example, leaf mass per area (LMA) is positively related to photosynthetic productivity and negatively to structural robustness and depends on resource availability and environmental conditions (Díaz et al., 2016; Grime, 1988; Poorter et al., 2009). Leaf pigments (e.g., chlorophyll, carotenoids) determine photosynthetic capacities and their variations can indicate changes in plant health due to stress (Feret et al., 2008; Zarco-Tejada et al., 2018, 2019; Berger et al., 2022). Other leaf constituents such as nitrogen and carbon are directly linked to biosphere-atmosphere cycles (de Bello et al., 2010) and are important to parameterize vegetation in Earth system models (Yang et al., 2015). A comprehensive set of quantitative trait measurements is thus desirable to understand the functioning of ecosystems.

Still, despite the efforts towards compiling field observations from a myriad of studies into global databases (e.g. TRY, Kattge et al., 2020), the available data are sparse in terms of geographical coverage, species and range of traits (Asner et al., 2015; Kattge et al., 2020). In this context, hyperspectral remote sensing data offer an efficient proxy to map plant traits (Cavender-Bares et al., 2020; Jetz et al., 2016). Such data enable repeatable and non-destructive optical observations using numerous platforms and sensors providing information on spectral reflectance across a wide range of the electromagnetic spectrum via continuous narrow bands. Given the mechanistic interactions of light with leaf and canopy traits (Billings and Morris, 1951; Gates et al., 1965; Kattenborn and Schmidlein, 2019; Ustin and Gamon, 2010), hyperspectral observations have a high potential to reveal plant traits over remote and large areas (Hank et al., 2019; Asner and Martin, 2016; Homolová et al., 2013; Singh et al., 2015; van Cleemput et al., 2018; Danner et al., 2021; Wocher et al., 2022). Recently launched and forthcoming hyperspectral space missions such as PRecursore Iper-Spettrale della Missione Applicativa (PRISMA, Cogliati et al., 2021), Environmental Mapping and Analysis Program (EnMAP, Guanter et al., 2015) and Surface Biology and Geology (SBG, Cawse-Nicholson et al., 2021) along with the higher-resolution proximal and airborne instruments, support this potential and will provide an unprecedented source of data. However, in view of the varieties of these hyperspectral data sources and potential applications, we are missing transferable retrieval methods across sensors, acquisition settings, ecosystems and plant functional types.

From a methodological perspective, available retrieval methods range from data-driven statistical methods to the inversion of radiative transfer models (RTM) to hybrid methods (see Verrelst et al., 2019 for a review). RTMs simulate the interaction of light with vegetation properties and thus their inversion can represent a promising approach for plant trait retrieval (Berger et al., 2018; Dorigo et al., 2007; Feilhauer et al., 2017, 2018; Jacquemoud et al., 2009). Yet, plant trait retrieval by RTM inversion is only possible for traits that are considered in the RTM itself. Moreover, RTM inversions are very sensitive to the RTM's configuration and thus have to be specifically parameterized for different vegetation types, canopy structures, phenological stages or use cases (Dorigo et al., 2007; Atzberger and Richter, 2012; Verrelst et al., 2013). Conversely, data-driven approaches automatically learn the statistical relation between the spectral data and plant traits. Partial Least Squares regression (PLSR) (Geladi and Kowalski, 1986; Wold et al., 2001) can be considered as the benchmark approach given its long history in imaging spectroscopy (Asner and Martin, 2008; Feilhauer et al., 2010; Singh et al., 2015; Wang et al., 2020). In recent years, new machine learning algorithms emerged as powerful approaches to solve retrieval tasks from hyperspectral data (Wang et al., 2020; Priliani et al., 2021; Shi et al., 2022).

Despite the potentials of data-driven methods, there are multiple constraints:

1) Commonly, data-driven models are trained with data sets representing limited variation in ecosystem properties, plant functional types, sensor systems and acquisition settings, thus limiting their transferability. For instance, previous studies (Asner et al., 2015; Berger et al., 2020; Wang et al., 2019) have concentrated on individual ecosystems

such as croplands, forests, or grasslands using specific data sets. However, models developed from these data sets may produce significant uncertainties when employed on a new data set, making them less transferable to other ecosystems or alternative data sets (Wang et al., 2020).

2) Data-driven models are often built independently for different traits. This prevents exploiting interrelationships between certain traits. For example, different traits may be driven by the same processes or may manifest in overlapping absorption features such as pigments or resource-investment related traits. Consequently, taking the trait interrelations into account might improve the overall retrieval quality. Moreover, the simultaneous prediction of multiple traits may also enlarge computational efficiency. It is thus compelling to aim for a data-driven approach that is capable of predicting a set of traits simultaneously. We further refer to such an approach as 'multi-trait' model.

3) Furthermore, most data-driven approaches for plant trait retrieval cannot easily be extended with new training data, which hinders continuous model improvements and knowledge transferability.

Deep learning and particularly Convolutional Neural Networks (CNNs) may pave new avenues to alleviate such issues (Sosnin et al., 2019; Yosinski et al., 2014; Zhang and Yang, 2021). CNNs are a powerful method for automatic feature engineering and are increasingly being applied to remote sensing data (Kattenborn et al., 2021; Zhu et al., 2017). Due to their depth and large number of neurons such models are capable of learning complex relationships. Accordingly, given sufficient representativeness of the input data, such models may learn transferable relationships across application domains, sensor types and acquisition settings. Moreover, CNNs are commonly trained iteratively, enabling to exploit very large data sets and allowing for continuous updating and fine-tuning of models with new, unseen data (Shin et al., 2016).

The availability of canopy spectra and their corresponding trait observations from different studies encompassing different plant types and sensors constantly increases (e.g. Rogers et al., 2021; van Cleemput et al., 2019). This opens a way to harness the scalability of deep learning and test the robustness of the models when integrating multi-source hyperspectral and plant trait data (e.g. EcoSIS, Wagner et al., 2018). However, due to the different context of these studies, a combination of such data sets is naturally sparse, meaning not all potential traits are covered across different data sets. Therefore, the objective of this study is to explore the potential of weakly supervised approaches to train models on sparse data for simultaneously predicting multiple traits ($n = 20$) from canopy hyperspectral data. This analysis is based on a combination of 42 data sets from heterogeneous data of different vegetation and sensor types. We implement three weakly-supervised multi-trait CNN approaches to investigate the hypothesis of whether the incorporation of trait-trait correlation in models' calibration would improve the trait estimations. The performance of these strategies is compared to common single-trait PLSR and single-trait CNN models.

2. Material and methods

2.1. Data merging and cleaning

We employed 42 data sets of full range canopy spectra (400–2500 nm) with corresponding trait measurements (e.g. LMA, pigments) that were available upon request or from archives (e.g. EcoSIS, PANGEA) (Burnett et al., 2021; Cerasoli et al., 2018; Chlus et al., 2020; Ewald et al., 2018b, 2020; Hank et al., 2015, 2016; Herrmann et al., 2011; Kattenborn et al., 2019a; Pottier et al., 2014; Rogers et al., 2021; Singh et al., 2015; van Cleemput et al., 2019; Wang et al., 2020; Wocher et al., 2018; Dao et al., 2021). The sites of the collected samples are distributed across different continents (America, Asia and Europe see Fig. A.1 in Appendix A) and vary in climate and vegetation type (see details Table A.1 in Appendix A). The data comprise observations from different natural and semi-natural ecosystems (forest, grassland, tundra and shrubland), agricultural sites (crops and pastures), as well as plant-pot-

experiments. Hence, the resulting data represent an aggregation of large and heterogeneous multi-site and multi-ecosystem sources.

2.1.1. Hyperspectral data

Canopy reflectance spectra were acquired with proximal and airborne hyperspectral sensors (e.g. ASD FieldSpec, Spectra Vista Corporation, SVC; AVIRIS; NEON Airborne Observation Platform AOP) and have different spectral properties. Still, they cover a comparable wavelength range of the solar electromagnetic spectrum (see Table A.1). A forward and backward linear interpolation was performed to unify the diverse measurements in the full range of 400–2500 nm in 1 nm steps. To deal with the known issues of atmospheric water absorption in open-sky canopy reflectance spectra, we removed water absorption regions (1351–1430, 1801–2050 and 2451–2501 nm) and independently smoothed the three remaining parts of the spectra with a Savitzky-Golay filter (Savitzky and Golay, 1964) using a window size of 65 nm. Finally, 1721 interpolated spectral bands were retained for the analysis. Given the heterogeneity of the different data sets, the 5573 processed spectra cover a wide range of reflectance values (Fig. 1). The data were checked for overall spectral artifacts or inconsistencies (Appendix B). Despite the heterogeneity in land cover and vegetation types, we observed smooth transitions between the spectral features of the different data sets originating from sensor or pre-processing procedures (Fig. B.1 in Appendix B).

2.1.2. Leaf and canopy traits

From the available reference data, we selected a variety of traits (Table 1) related to light harvesting and growth, e.g. leaf pigments, nitrogen, structure and resource investments, leaf area index (LAI), equivalent water thickness (EWT) and leaf mass per area (LMA). Where necessary, leaf traits were converted to area basis, in contrast to mass-based measurements, to avoid the high correlation with LMA (see also Fig. B.2 in Appendix B) and to facilitate the model to learn the actual absorption features of the respective constituent (Hill et al., 2019; Kattenborn et al., 2019b; Ustin and Gamon, 2010; Zhao et al., 2021) (Fig. B.2). Main conversions were based on the common relationships from literature (Kattenborn and Schmidlein, 2019; Lichtenthaler, 1987) (Table A.2 in Appendix A). Table 1 summarizes the quantity of observations for each trait, their value ranges and the number of associated data sets. For the further analyses and for the sake of the training stability and computational efficiency, the trait values were rescaled. For this, we used the power transformation, which is a monotonic transformation to transform and normalize the data to a more-Gaussian-like distribution.

2.2. Multi-trait model development

2.2.1. CNN implementation and training

Given the one-dimensional nature of the spectral data, we used one-dimensional Convolutional Neural Networks (1D-CNN). The context of

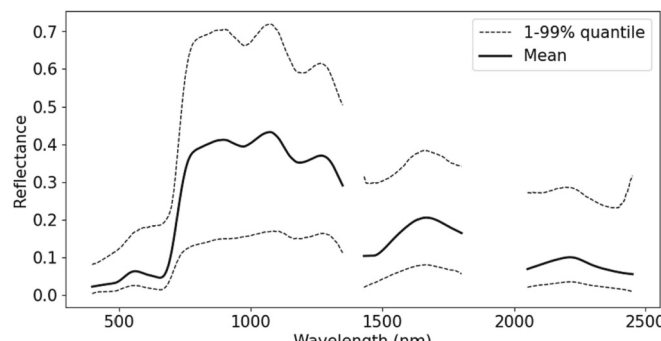


Fig. 1. Distribution of canopy reflectance of the available samples ($N = 5573$).

neighboring wavelengths of the spectra makes CNN-based models preferable here to the naive multilayer perceptron architecture (MLP). CNNs can have a deep structure and conventionally include blocks (convolutional block) of successive layers including convolution, pooling, and activation layers. The convolution operation is a sliding dot product of a filter (kernel) applied to the spectral signal. Several filters are used in the convolutional layer where they serve as a feature extractor and are iteratively learned during the CNN training process. The kernel's sliding fashion enables feature detection to be applied across the full signal range. Subsequently, the pooling layers enable to condense information from the output of the convolutional layers and facilitate a hierarchical feature extraction at multiple wavelength scales. For more details about CNNs, the reader is referred to Goodfellow et al. (2016).

As backbone architecture, we used an adapted version of EfficientNet-B0 (Tan and Le, 2019), which is modified for one dimensional input data. EfficientNet architectures are composed of a sequence of the previously described CNN blocks with skip connections. They are designed to improve accuracy and efficiency by using a scalable structure that allows the network to learn effectively from larger resolutions while reducing computation costs. This is done through a combination of depthwise separable convolutions, 1×1 convolutions and network scaling methods (Tan and Le, 2019). The output layer of the implemented architecture comprised 20 units corresponding to the number of traits to be predicted.

The learning process of the model was based on the stochastic gradient descent algorithm, where the Adaptive Momentum estimation (Adam) optimizer was used to update the weights (Kingma and Ba, 2014). The number of epochs was set to 300 with a batch size of 32. We employed the Hubert loss function to reduce the effect of outliers. Given sparsity and resulting imbalance of trait observations in the merged data set, we used a weighted loss version. The weights of the samples w (%) were calculated for each sample as the complement of the number of non-null trait samples n_{nn} to the total number of samples n_{tot} in the corresponding original data set (Eq. 1). Additionally, a random up-sampling with replacement was performed to have an equal number of samples from each data set on the training set.

$$w = 100 - (n_{nn}/n_{tot})^* 100 \quad (1)$$

To avoid over-fitting, two conventional regularization techniques were used: data augmentation and drop out. Data augmentation introduces artificial variation in the data to help regulate the learning process. We applied two random modifications for every epoch (a training cycle using all observations) with a 15% chance. This included 1) an addition of random noise with $\pm 30\%$ of the spectral standard deviation per wavelength derived from all training samples and 2) an amplitude multiplication of the entire reflectance spectra with a random value between 0.98 and 1.02. As additional model regularization, we applied dropout (Hinton et al., 2012) after each block, which randomly drops learning units with a defined probability.

Within the 300 epochs, we selected the final model according to the lowest root mean squared error of a 20% hold-out from the training data. All CNN models were implemented in Python (3.9.5) with the TensorFlow (2.7.0) and Keras (2.7.0) frameworks.

2.2.2. CNN multi-trait and weakly supervised learning

In the view of the sparsity of the merged data set (Table 1), we tested three different strategies to train multi-trait models using the above-mentioned CNN architecture: The first strategy, CNN_{multilncomplete}, was trained on the original sparse data set. To overcome data sparsity, we modified the loss function to only update the weights according to traits where a corresponding reference observation was present (i.e. not a missing value). This approach falls within the incomplete supervision category in the context of weakly supervised learning (Zhou, 2018). This strategy is considered as the baseline approach in this study.

Table 1

Statistics of 20 selected functional traits available across 42 data sets. More details on the data sets can be found in Table A.1. N = Number of samples, N Data sets = Number of data sets including the trait, Std = standard deviation, Min = minimum, Max = maximum.

Trait name	Trait description	Unit	N	N Data sets	Mean	Std	Min	Max
Anth	Anthocyanin content	($\mu\text{g}/\text{cm}^2$)	644	2	1.27	0.41	0.56	2.98
Boron	Boron content	($\mu\text{g}/\text{cm}^2$)	1086	14	0.39	0.26	0.01	2.34
C	Carbon content	(mg/cm^2)	1876	23	5.84	4.44	0.10	37.29
Ca	Calcium content	($\mu\text{g}/\text{cm}^2$)	1045	16	107.25	101.97	0.69	988.73
Car	Carotenoid content	($\mu\text{g}/\text{cm}^2$)	1859	21	8.75	2.77	1.18	40.44
Cellulose	Cellulose	(mg/cm^2)	1402	15	2.35	1.87	0.35	15.22
Chl	Chlorophyll content	($\mu\text{g}/\text{cm}^2$)	2141	24	38.57	14.53	4.45	229.50
Copper	Copper content	($\mu\text{g}/\text{cm}^2$)	1101	14	0.07	0.03	0.01	0.28
EWT	Equivalent Water Thickness	(mg/cm^2)	1918	19	15.65	9.27	0.23	80.62
Fiber	Fiber	(mg/cm^2)	1385	15	5.23	4.57	0.14	29.81
LAI	Leaf Area Index	(m^2/m^2)	1643	15	3.35	1.64	0.06	7.67
Lignin	Lignin	(mg/cm^2)	1415	16	2.69	2.41	0.05	14.58
LMA	Leaf Mass per Area	(g/m^2)	3328	32	92.05	68.08	5.72	663.81
Magnesium	Magnesium content	($\mu\text{g}/\text{cm}^2$)	1099	15	24.09	16.16	0.25	141.54
Manganese	Manganese content	($\mu\text{g}/\text{cm}^2$)	894	14	3.09	2.31	0.01	15.19
N	Nitrogen content	(mg/cm^2)	2193	26	0.19	0.10	0.01	0.95
NSC	Non-Structural Carbohydrates	(mg/cm^2)	1093	14	3.21	2.85	0.28	21.83
Phosphorus	Phosphorus content	($\mu\text{g}/\text{cm}^2$)	1289	16	14.42	9.45	0.29	73.43
Potassium	Potassium content	($\mu\text{g}/\text{cm}^2$)	1008	15	102.64	62.73	0.40	470.07
Sulfur	Sulfur content	($\mu\text{g}/\text{cm}^2$)	1039	14	13.31	9.13	0.62	57.23

The second strategy, CNN_{multiInexact} aims to maximize the identification of trait-trait relations during the learning process from all data samples and, hence, includes a gap-filling of missing trait values. The gap-filling process is based on the predictions of the CNN_{multiIncomplete}. To avoid unrealistic values, trait predictions lower than the 1% quantile and exceeding the 99% quantile of the original data set (Table 1) were not considered for gap-filling. This automated gap-filling approach does not require data on species or ecosystem characteristics, which might be missing or hard to define (Schrodt et al., 2015; Shan et al., 2012). Instead, it directly learns trait-trait relationships from available hyperspectral data. CNN_{multiInexact} falls within the two weak supervision categories: incomplete and inexact supervision. The incomplete supervision is related to the gap-filling procedure, and the inexact supervision is performed when training on the completed but noisy labels (i.e. reference data with gap-filled values).

The third strategy, CNN_{multiIncompleteTRY} aims to fill data gaps with trait observations obtained from the TRY plant trait database (Kattge et al., 2020). The TRY database (version 5), includes >11.8 million trait observations across >270.000 taxa. For each dominant species found in the reference data, trait observations were queried from TRY using the species name. We applied fuzzy matching to deal with minor inconsistencies in the spelling of the species names with a Damerau-Levenshtein-Edit distance >89 (Damerau, 1964; Konstantinidis, 2005). The dominant species mapping resulted therefore in 144 correspondences with TRY species. For these species, the median trait values were then used to fill the missing values. This gap-filled data set was then used to train the multi-trait CNN model (CNN_{multiIncompleteTRY}). This strategy falls also within the inexact and incomplete weak supervision categories as the model is trained on sparse and noisy labels (i.e. median trait values within species).

2.3. Comparison to single-trait models

To evaluate the benefit of the multi-trait models and the uncertainty introduced from the weakly supervised approaches (i.e. inexact and incomplete), we additionally trained single-trait CNN (CNN_{single}) models, where a separate model was trained for each individual trait. Apart from the final layer (number of output units), the architecture for these models was the same as for the multi-trait models (Section 2.2.1). Moreover, we compared the CNN-based single and multi-trait models to partial least squares regression (Wold et al., 1984). PLSR is currently one of the most frequently applied algorithms for imaging spectroscopy (Feilhauer et al., 2010; Homolová et al., 2013). For training PLSR

models for each trait (PLSR_{single}), we used scikit-learn (version 0.24.2) Python libraries. To avoid over-fitting, the optimal PLSR number of latent components was selected by minimizing the predicted residual sum of squares (PRESS) in cross-validation (Chen et al., 2004).

2.4. Model evaluation

Using trait measurements and the canopy reflectance data from 42 data sets described in Section 2.1, we compared the predictive performance of the 1) multi-trait CNN models to 2) single-trait CNN and 3) single-trait PLSR models (Fig. 2). For a fair comparison, the same input data settings were adopted for the training and evaluation of all modeling approaches including data splitting, transformation and up-sampling. The up-sampling procedure is a random sampling with replacement and was applied to all samples in the training set to make sure that a comparable number of samples is included from each data set and to reduce the effect of bias towards data sets with more samples.

After training, the models were evaluated for their performance 1) within the domain of the training data (internal validation) using randomly sampled hold-outs, and 2) with regard to their transferability to new domains (external validation), where each individual data set was once retained from model training. For the internal evaluation, we adopted a 5-fold cross-validation (CV) for all models. Given the unbalanced sampling frequency of the individual data sets, we performed a stratified cross-validation based on the data set provenance (original data sets). This procedure ensures equal distribution of trait samples across the folds. For the hold-out test sets, only the original (and not the gap-filled) samples were used. The external validation consisted of training the models repetitively on 41 out of 42 data sets while keeping one data set as hold-out for testing. To reduce computational load, the data set-CV was only applied for CNN_{multiIncomplete} and PLSR_{single}. We evaluated the model performances using the coefficient of determination R² and the normalized root mean squared error (nRMSE, %). The nRMSE was derived by normalizing the root mean square error over the range of the observations (1–99% quantile). The final model performance was obtained by averaging the R² and nRMSE values over the 5 folds of the CV.

2.5. Feature attribution

To visualize the spectral features learned by the CNN_{multiIncomplete} model, we estimated the feature importance of each input wavelength, which were interpreted and compared with known spectral plant

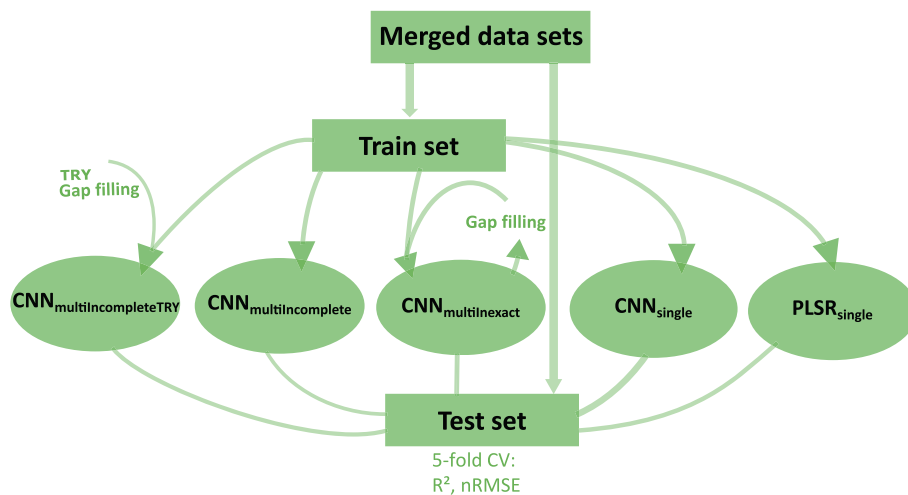


Fig. 2. Model performance assessment (internal validation) of multi-trait and single-trait models. The evaluation is based on a stratified 5-fold cross-validation.

features. As feature importance metrics, we derived medians of Shapley Additive exPlanations (SHAP, [Lundberg and Lee, 2017](#)) absolute values. The SHAP values present a unified approach to explain model predictions based on the optimal game theory Shapley values. The Shapley values represent the local marginal contribution (i.e. for individual samples in the data) of each feature in the input for a specific prediction. They attribute the change in the expected model prediction when conditioning on one feature by calculating the difference from the prediction in which the feature in question is not included ([Lundberg and Lee, 2017](#)). These values can be approximated with different algorithms. We used the gradient explainer class, which combines the integrated gradients ([Sundararajan et al., 2017](#)), SHAP and SmoothGrad ([Smilkov et al., 2017](#)) methods. All SHAP coefficients were rescaled between 0 and 1 and normalized by the mean SHAP value of all traits to eliminate the effect of the learned trait covariance. For comparison, we also displayed the PLSR regression coefficients.

2.6. Uncertainty estimation

As indicated by earlier studies, transferability of machine learning-based models to new, unseen data depends on the distance in feature space (Kattenborn et al., 2022; Ludwig et al., 2023; Mila et al., 2022). Therefore, we implemented an uncertainty estimation procedure to reveal the effect of spectral dissimilarity between new data and data used in model training. Such a procedure is particularly valuable in view of large-scale mapping across ecosystems and sensors.

Inspired by [Janet et al. \(2019\)](#) and [Meyer and Pebesma \(2021\)](#), the implemented uncertainty estimation was based on the relationship between 1) CNN model residuals obtained from the internal evaluation and 2) the distance in feature space (dissimilarity of training vs. test sets). To reveal spectral dissimilarity from the eye of the CNN, the feature space was obtained from the CNN model embedding space of the global pooling of the last convolutional layer. Based on this feature space, the dissimilarity for each test sample was calculated as the average distance to the five nearest neighbors of the training data. The model uncertainty was then estimated using the calculated dissimilarity as predictor in a 95% quantile regression. The predicted values can be seen as the worst-case error prediction of the model. This procedure was tested for the `CNNmultiIncomplete` model.

3. Results

3.1. Summary of the merged data set

3.1.1. Trait variations

The trait values across the merged data sets varied highly due to the heterogeneity in vegetation types and species (Table 1). This yields a large range in the trait values. LMA, Chl and EWT showed the highest variability (Coefficient of Variation CV = 47.97, 42.91, 38.44%, see Fig. B. 3, 4 in Appendix B) in the original data while all other traits had similar variations (on average 35%). The correlation analysis based on Spearman coefficient of the merged data set revealed high correlation between several traits (Fig. 3). As expected, leaf constituents related to plant resource investments showed a large correlation (e.g. LMA, Carbon, Lignin, Fiber, Cellulose). These resource-investment related traits were rather independent from leaf pigments, which in turn were highly correlated among each other (Chl, Car, Anth). Both resource investment related traits and pigments showed a considerable correlation with leaf N. Overall, rather weak correlations were found for LAI and leaf constituents, whereas for N and C a positive relationship was observed. Water content overall also showed a positive correlation with other leaf constituents.

3.1.2. Canopy spectra

The canopy reflectance spectra were relatively similar when averaged across land cover types (Fig. 4) and we found smooth transitions across data sets and biomes (Fig. B.1, Appendix B). Higher reflectance values were observed for the Tundra data in the NIR region (Fig. 4a). Largest coefficients of variations were found in the SWIR 2 region (2000–2500 nm) followed by the VIS region (400–750 nm). Most of the spectral variation was found in the crop related samples whilst forest samples had the lowest spectral variation (Fig. 4b).

3.2. Trait predictions

3.2.1. Prediction performances

The model performances derived from the 5-fold cross-validation showed the overall predictive performance varied greatly for the different traits (Fig. 5). With all CNN-based models, the goodness-of-fit of the predictions was higher for LMA, C, NSC (Non-structural carbon) ($R^2 > 0.69$). Lower predictive performances of these models were obtained for EWT, N, Pigments, LAI, Cellulose, Lignin, Fiber, Copper and Phosphorus (R^2 : 0.46–0.69 and nRMSE: 12–17%). Overall, the trait estimation performances of the CNN-based models exceeded those of the PLSR models (R^2 : 0.18 to 0.66 and nRMSE: 11–22%). The PLSR models

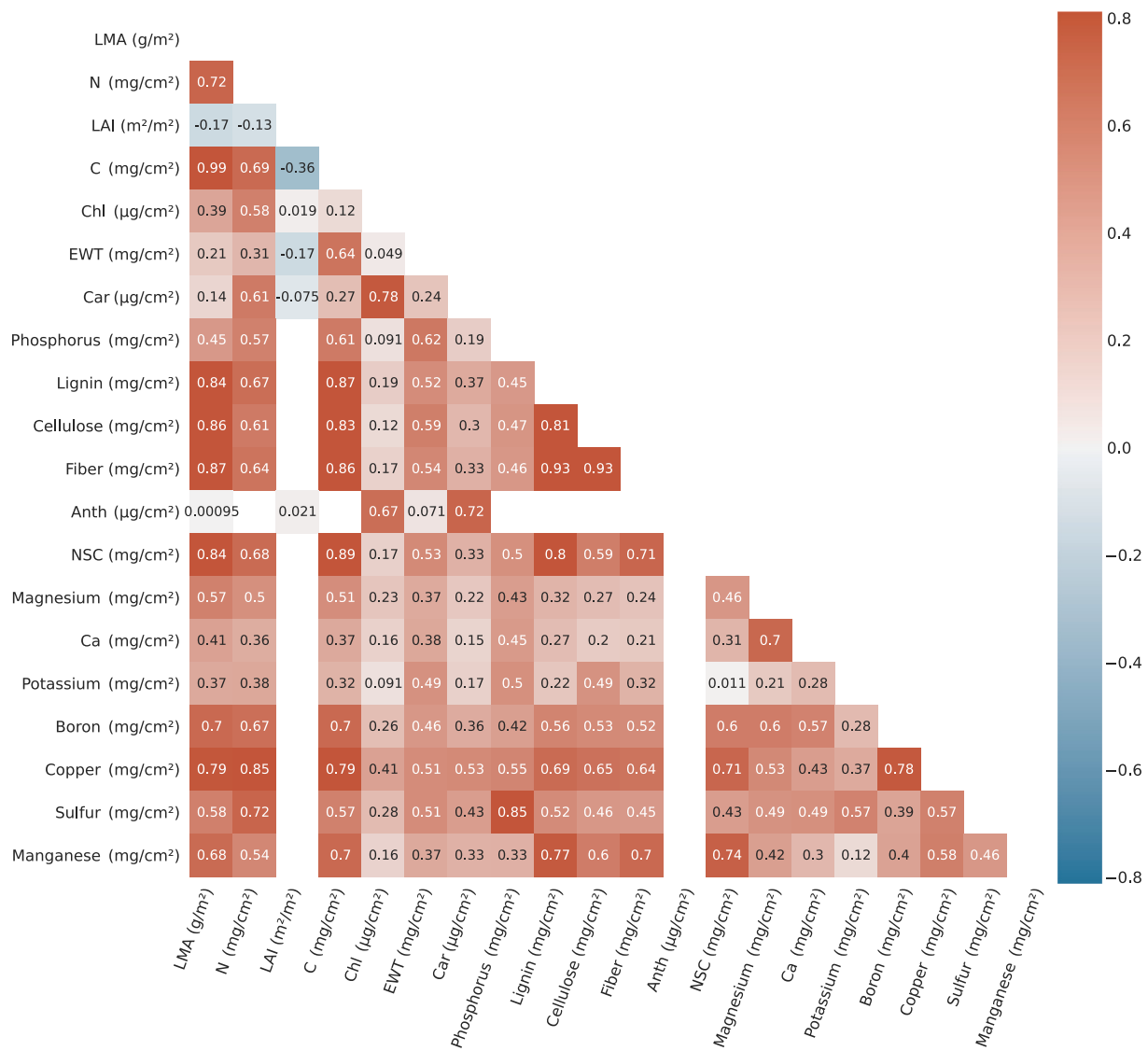


Fig. 3. Correlation plot of traits based on Spearman's rank correlation coefficient. Refer to Table 1 for an explanation of the traits. A correlation of leaf traits on a mass-basis is given in Fig. B.2.

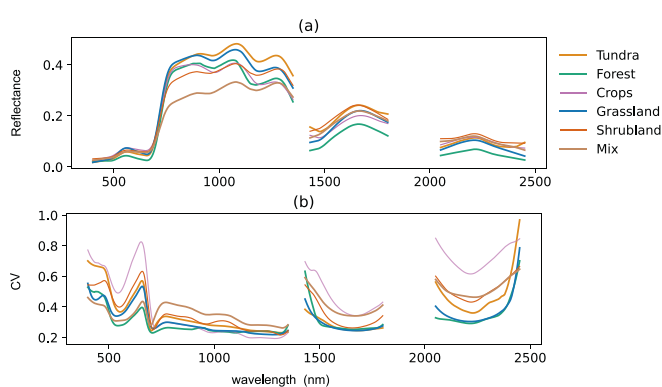


Fig. 4. Canopy average reflectance and the corresponding spectral variation (Coefficient of Variation, CV) across the different land cover types.

showed bias with high values for some traits, including LMA, Pigments and Carbon related traits (see Fig. D.1). Only for a few traits, i.e. Boron, Ca and Manganese, the PLSR models showed higher performances than CNN models. Ca, Boron, Magnesium, Sulfur, Potassium and Manganese

obtained the lowest validation performance for all models, especially with single-trait models ($R^2 < 0.44$ and $nRMSE > 15\%$).

According to a Wilcoxon signed-rank test, the multi-trait models performed significantly better than single-trait models across all traits (e.g. $\text{CNN}_{\text{multiIncomplete}} p < 0.001$, $w = 205$, details see Appendix C). In comparison to $\text{CNN}_{\text{single}}$, CNN-based, multi-trait models clearly improved the prediction performance for most of the traits. The prediction performance was particularly improved for traits where fewer samples were available or where a comparably lower correlation with spectral bands was observed (Fig. B.4, Appendix B), including Anth, Sulfur, Ca and Potassium (Fig. 5b). Overall, the R^2 across all traits was higher for CNN multi-trait models than for $\text{CNN}_{\text{single}}$ except for LMA, C and NSC (Fig. 5c, d).

Similar performance was obtained among the different CNN-based multi-trait models, i.e. $\text{CNN}_{\text{multiIncomplete}}$, $\text{CNN}_{\text{multiInexact}}$ and $\text{CNN}_{\text{multiIncompleteTRY}}$. The predictive performance for the $\text{CNN}_{\text{multiInexact}}$ ranged from R^2 of 0.21–0.70 and $nRMSE$ of 10.41–18.79%, for $\text{CNN}_{\text{multiIncomplete}}$ R^2 of 0.29–0.77 and $nRMSE$ of 9.17–17.81% and $\text{CNN}_{\text{multiIncompleteTRY}}$ R^2 of 0.29–0.78 and $nRMSE$ of 8.92–17.85%. Overall, the $\text{CNN}_{\text{multiIncompleteTRY}}$ performed slightly better than the other two multi-trait strategies for most of the traits (Fig. 5). The $\text{CNN}_{\text{multiIncompleteTRY}}$ procedure is further discussed in Section 3.2.2.

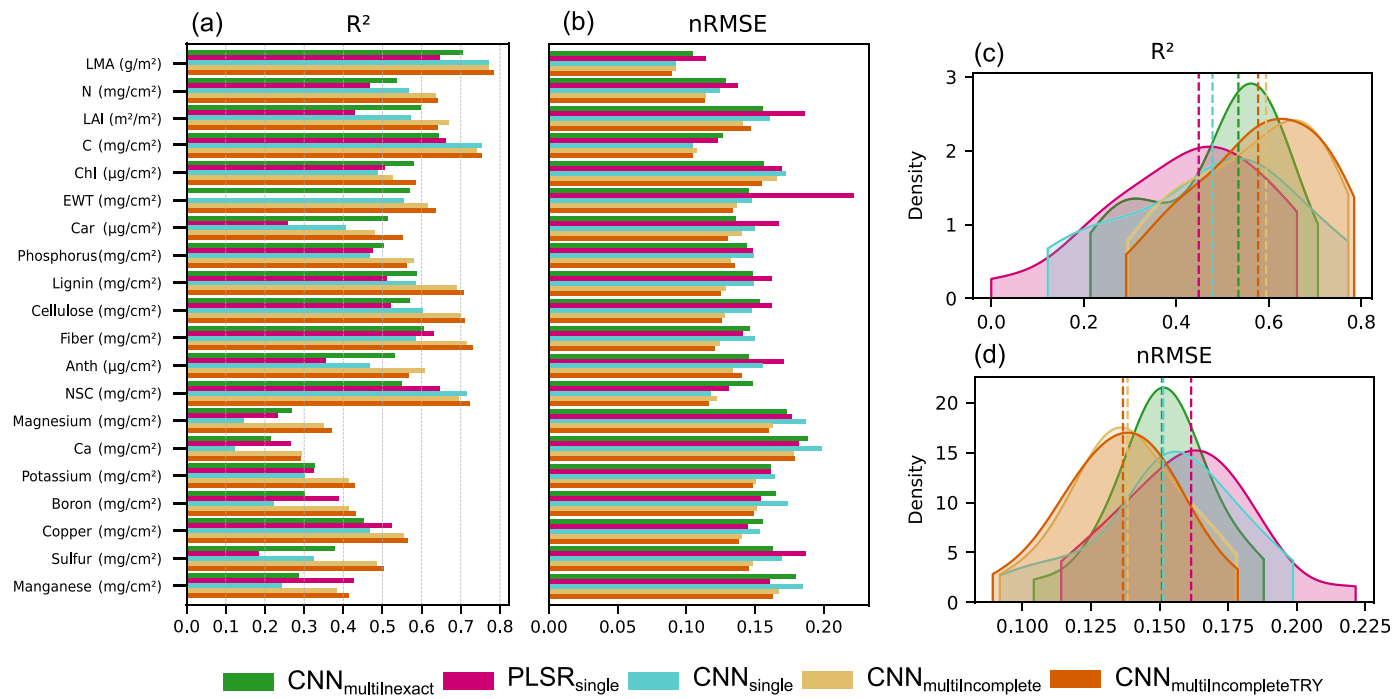


Fig. 5. (a) and (b): Comparative predictive accuracies (R^2 and nRMSE) from the stratified 5-fold cross validation of the CNN_{multincomplete}, CNN_{multinexact} and CNN_{multincompleteTRY} models as well as PLSR_{single} and CNN_{single} models for 20 traits. (c) and (d): The kernel density estimate (KDE) of the trait-based metric distributions (R^2 and nRMSE) with the associated median values (dashed lines). Refer to Table 1 for an explanation of the traits. Detailed performances can be found in Table C.1 and 2 Appendix C.

All multi-trait approaches resulted in relatively robust and similar prediction performances across the different vegetation types (Fig. 6, D.3, 4 Appendix D). For some traits (e.g. LMA, N, EWT), the values are slightly clustered according to vegetation types, but we did not observe a prominent or systematic bias in predictive performance across these classes. For most traits, the model predictions are evenly scattered around the 1:1 line, which is also underlined by slopes of the linear fit close to 1 between the predicted and observed trait values (Fig. 6, D.3, 4 Appendix D).

Similar performance results were followed with the external evaluation, where CNN multi-trait model surpassed the performance of PLSR_{single} models (Fig. 7, E.1 Appendix E). With both modeling approaches, the performance across all traits with the external validation was lower than the internal validation, especially with PLSR_{single} (Fig. 7, E.1, Table E.1). For CNN_{multincomplete} LMA and C were the most transferable traits with R^2 higher than 0.6 which is consistent with the internal validation, while for PLSR Copper and Chl had the highest goodness-of-fit with $R^2 > 0.39$. However, the baseline multi-trait model (CNN_{multincomplete}) showed a bias in high trait values with N and LAI for example.

3.2.2. Details on trait database integration

Due to data availability, the gap-filling of the CNN_{multincompleteTRY} procedure was limited to 13 out of 20 traits (Table 3). The model performance significantly improved for all the gap-filled traits ($p = 0.004$, $w = 82$, Wilcoxon signed-rank test). Surprisingly, the CNN_{multincompleteTRY} approach resulted even in significantly improved performance for traits where no gap-filling could be performed, i.e. EWT, Car, Fiber, NSC and S ($p = 0.0313$, $w = 15$). While the filling rate was not an important factor for model improvement, the introduced variation from the species-based trait values had the largest effect on traits that already had less sparse trait observations samples in the data set. For instance, Chl had the highest improvement in performance and even surpasses the results of the baseline model CNN_{multincomplete} (Table 3).

3.2.3. Feature importance

The feature importance for CNN_{multincomplete} and PLSR_{single} showed a clear correspondence in the overall patterns (Fig. 8). For LMA, the relevant wavelengths in the CNN multi-trait model were spread across the entire spectrum, with higher values in the longer wavelengths of the NIR and SWIR regions (1200–2450 nm). As expected, very similar patterns were found for traits that directly contribute to LMA, namely C, Cellulose, Fiber and Lignin. The CNN multi-trait estimation of Chl and Car mostly relied on spectral bands in the VIS and red-edge region (approx. 500–800 nm). For LAI, high SHAP values were found in the NIR region.

4. Discussion

4.1. Considerations on the merged data set

The transferability of statistical models to predict plant traits from new reflectance spectra is a major challenge (Ainsworth et al., 2014; Heckmann et al., 2017; Silva-Perez et al., 2018). Few previous studies have demonstrated that the transferability of models can be enhanced when the model training includes plots from different species and sites (Asner et al., 2015; Serbin et al., 2019; Wang et al., 2020; Kothari et al., 2022b). Here, we merged 42 canopy reflectance data sets (from 28 studies) to assess the robustness of retrieval models when calibrated on heterogeneous data not only from different ecosystem types but also experimental settings (e.g. hyperspectral data acquisition and in-situ measurement protocols). This procedure provides an opportunity to address common shortages of reference data while also increasing the representativeness in terms of geographical coverage and diversity in vegetation type in the training data. Yet, it should be noted that the temporal coverage of the data is biased towards the peak of the vegetation period, while the senescence is underrepresented. This may affect for example the inter-correlations between traits as displayed in Fig. 3.

Merging the data sets required expert knowledge and a considerable effort for checking, cleaning, and converting trait observations.

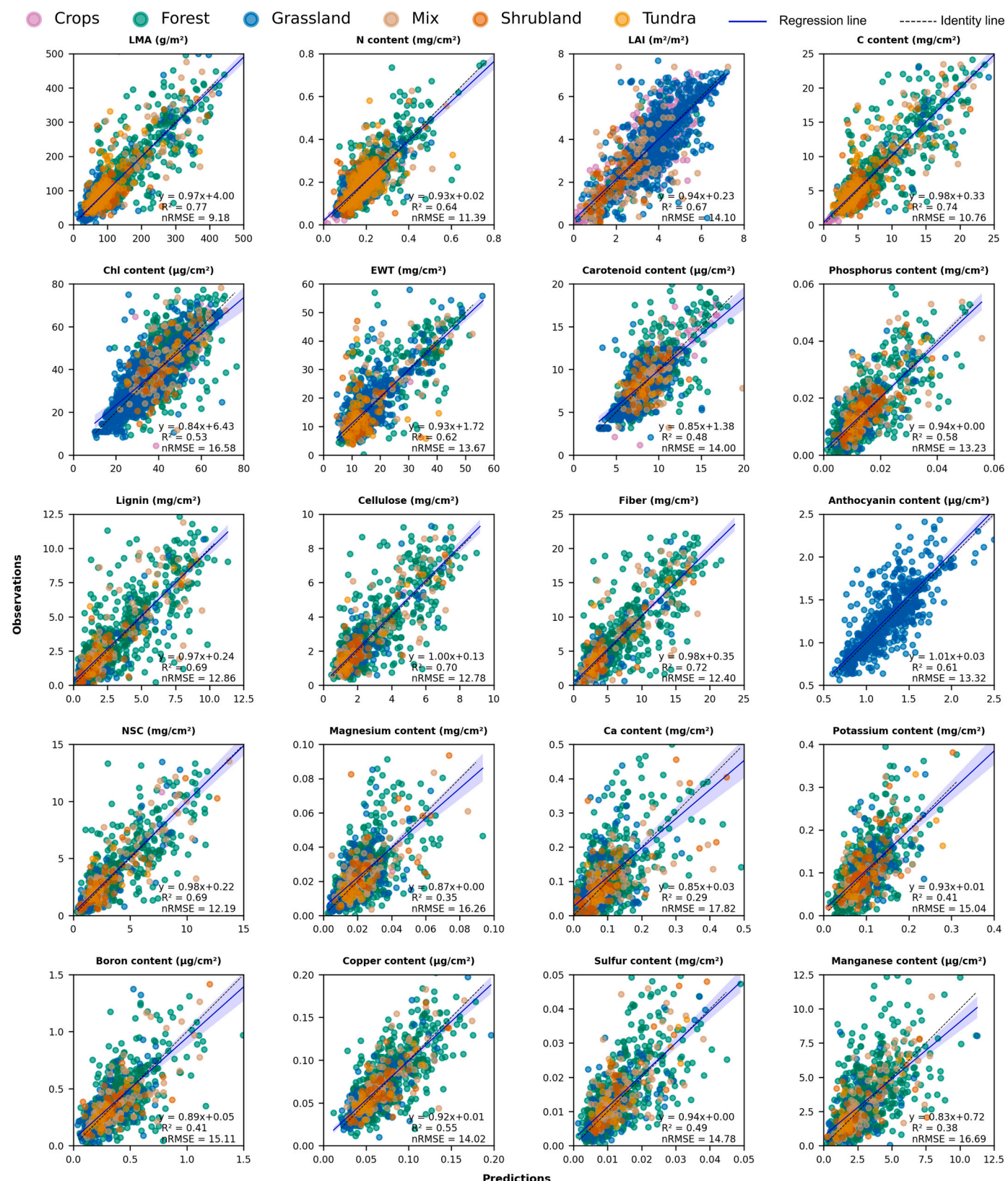


Fig. 6. Internal validation: Correlation between observed and predicted values of 20 traits from the multi-trait model $\text{CNN}_{\text{multiIncomplete}}$. The shown vegetation types only refer to the available types in the original associated data sets (not all land cover types are covered for each trait). Refer to Table 1 for an explanation of the traits. Scatter plots for the other models are given in Appendix D.

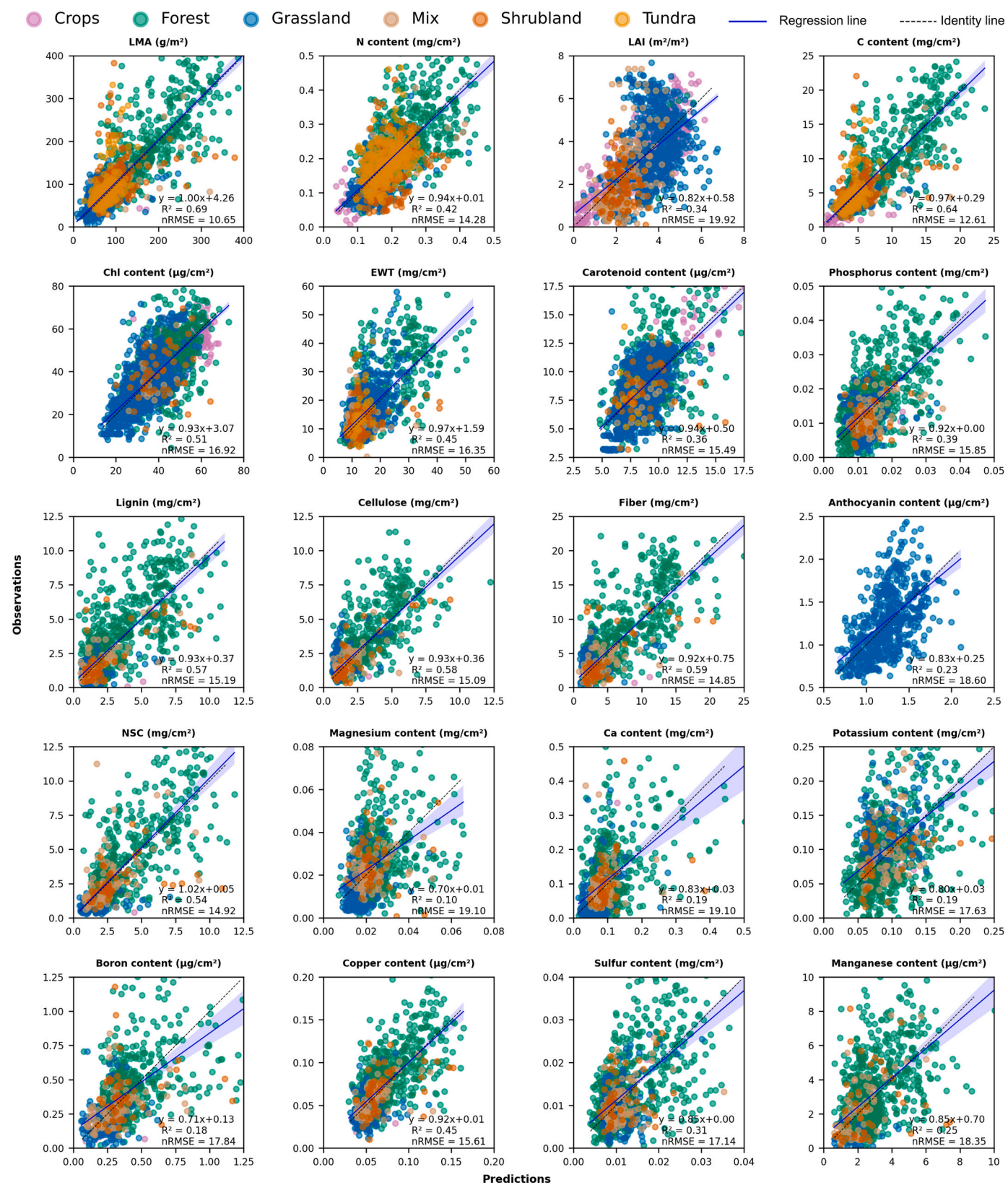


Fig. 7. External validation: Correlation between observed and predicted values of 20 traits from the multi-trait model $\text{CNN}_{\text{multiIncomplete}}$. The shown vegetation types only refer to the available types in the original associated data sets. Scatter plots for $\text{PLSR}_{\text{single}}$ are given in Appendix E.

Table 3

Comparative nRMSE values (%) of the $\text{CNN}_{\text{multiIncompleteTRY}}$ with $\text{CNN}_{\text{multiIncomplete}}$ and $\text{CNN}_{\text{single}}$ models. $\text{CNN}_{\text{multiIncompleteTRY}}$. Filling rates = (n obs. after - n obs. before) * 100 / n obs. before. Refer to Table 1 for an explanation of the traits and to Table C.3 for more detailed metrics (Appendix C).

Traits	Filling rate (%)	nRMSE (%) $\text{CNN}_{\text{single}}$	nRMSE (%) $\text{CNN}_{\text{multiIncomplete}}$	nRMSE (%) $\text{CNN}_{\text{multiIncompleteTRY}}$
Potassium	118.14	16.42	15.04	14.84
Phosphorus	99.07	14.89	13.23	13.51
Ca	97.42	19.87	17.82	17.85
Magnesium	93.64	18.65	16.26	16.00
C	92.33	10.45	10.76	10.48
Manganese	64.54	18.49	16.69	16.26
N	50.69	12.40	11.39	11.29
Copper	50.27	15.29	14.02	13.83
Chl	34.13	17.25	16.58	15.50
LMA	23.20	9.18	9.18	8.92
Lignin	12.43	14.91	12.86	12.48
Cellulose	7.77	14.71	12.78	12.58
Boron	0.55	17.39	15.11	14.86

Although a large share of the data used here was acquired from the EcoSIS database, the available data often include errors and inconsistencies, e.g. assignment of wrong dimensions or units. In consideration of future initiatives for data integration, these experiences emphasize the need for a harmonization of plant trait observations, including units and dimensions, e.g. area or mass based, as well as quality assessments, terminology and sampling protocols.

As this merged data set incorporates various ecosystems and land cover types, its trait variability exceeds those of previous studies (Table 1, Fig. 3, Asner et al., 2015; Schiefer et al., 2021; Serbin et al., 2019; Wang et al., 2019, 2020). We assume that merging the different data sets is a compelling requirement for developing models that are transferable and robust across different traits, ecosystems, and vegetation types in the context of global mapping. Here, the baseline multi-trait model ($\text{CNN}_{\text{multiIncomplete}}$) appeared to generalize well over the individual data sets (Fig. 7). It should be noted, however, that the data only represent a small portion of the Earth's flora and its spatio-temporal variation. Hence, despite the unprecedented trait variability realized here, the presented study should be regarded as a pioneering study in terms of model transferability and performance.

In the merged data set, not only the trait values but also the reflectance data showed considerable variability, which could be attributed not only to the spectral properties of the vegetation itself but also to differences in pre-processing modes with related uncertainties (e.g. during atmospheric correction procedures), remote sensing data acquisition settings (e.g. sun-observer-relationship) and instruments (e.g. airborne vs. field spectrometer data). We could not investigate in depth to what extent such factors limited the transferability of the models as information on such factors was not available for all individual data sets. Yet, we did not observe a significant difference in performance of our baseline multi-trait model ($\text{CNN}_{\text{multiIncomplete}}$) across the different remote sensing platforms ($p = 0.17$, $u = 72$, Mann-Whitney-U test) (Fig. E.3, 4 in Appendix E).

Merging data from multiple sources may improve model performances and transferability, but the sparsity and imbalance of trait observations challenged the model evaluations. For example, the number of data sets per trait ranges from 2 to 32 (Table 1), as most studies are application-specific and, hence, trait-specific. Likewise, the number of observations per data set ranged from 22 to 549. Thus, the relative performance of the model for the different traits is not necessarily directly comparable. Similarly, for some ecosystems or vegetation types only a few samples were available, which limited a conclusive performance evaluation in this regard. These challenges are expected to be resolved as more data may become openly available in the future.

4.2. Comparison of modeling approaches

Overall, the model performances of CNN-based models outperformed the widely used PLSR based models. This is consistent with previous studies that used hyperspectral data to retrieve vegetation and soil properties (Cui and Fearn, 2018; Ng et al., 2019; Pullanagari et al., 2021). The increased performance of CNN over PLSR may be explained by its ability to represent nonlinear relationships with an overall increased number of parameters, enabling the algorithm to learn more complex relationships. For example, the large trait-ranges of the merged data set presented in this study may inherit several non-linearities between spectra-trait-relationships. Such nonlinearities may result from saturation effects, where a change in high trait values results in little change of spectral reflectance, as observed in the present study for chlorophyll, LMA or LAI. The linearity of PLSR models appeared to be less suitable to resolve such effects, as indicated by a clear saturation of PLSR-based predictions for high values for these traits (Fig. D.1, E.1 in Appendix D and E). In such cases PLSR models tended to include more predictors (latent vectors) but this did not necessarily improve the model performance. Similar issues with PLSR-based models and saturation effects were also reported with leaf-scale reflectance data in Kothari et al. (2022). In contrast to the PLSR-based predictions, the predictions of the CNN models did not show saturation effects and no obvious systematic biases could be observed across the trait range (Fig. D.2–4).

In addition to the model performance, CNNs are known to be less reliant on feature engineering and are effective to identify automatically relevant features from the input data (Goodfellow et al., 2016). Previous studies in the context of variable retrieval from hyperspectral data showed that shallower machine learning methods were more dependent on pre-processing of input data (Cui and Fearn, 2018; Ng et al., 2019). Another advantage of CNNs and other batch-compatible deep learning methods over previous machine learning methods (e.g. PLSR, Random Forest) is that the data are exposed iteratively to the model, which potentially enables training models with an infinite amount of data without exceeding the memory. The latter aspect may become very relevant in the near future that promises an increase in data availability, e.g. via more data acquisitions from spaceborne spectrometers and a growing culture of open data through initiatives such as ecosis.org.

The multi-trait CNN models clearly outperformed the single-trait models. This is consistent with other studies in different areas which employed multi-task CNN models (Ng et al., 2019; Padarian et al., 2019; Ramsundar et al., 2015; Tsakiridis et al., 2020). In comparison of the $\text{CNN}_{\text{single}}$ model the retrieval of pigments, N, LAI, EWT, Phosphorus, Lignin, Cellulose, Fiber, Magnesium, Ca, Potassium, Boron, Copper, Sulfur was improved with our baseline multi-trait model ($\text{CNN}_{\text{multiIncomplete}}$). Even for traits that were only represented in a few data sets, the multi-trait models performed better than the single-trait models (e.g. Anth, Sulfur, Copper, Boron, Magnesium). We assume that multi-trait models not only allow for simultaneous and thus efficient trait retrieval, but also allow the model to indirectly learn trait-trait relationships.

Such trait-trait relationships may also explain the observed feature importances (Fig. 8). For instance, the spectral features for N were consistent with known protein features in the SWIR region (Féret et al., 2021) and others near the red-edge region related to pigments (Ustin et al., 2009). As expected, we also observed very similar spectral features across all wavelengths among traits related to leaf resource investments (LMA, Lignin, Fiber, Cellulose, and C; compare Kokaly et al., 2009), which may also explain higher model performance for several of these traits when predicted in a multi-trait setting. For Anth, we observed relatively accurate predictions and rather broad absorption features, although previous studies revealed that Anth pigments have rather subtle and narrow spectral absorption properties (Féret et al., 2017). We assume that the broad features obtained here result from the high correlation with Chl and Car (Fig. 3), which in turn have more

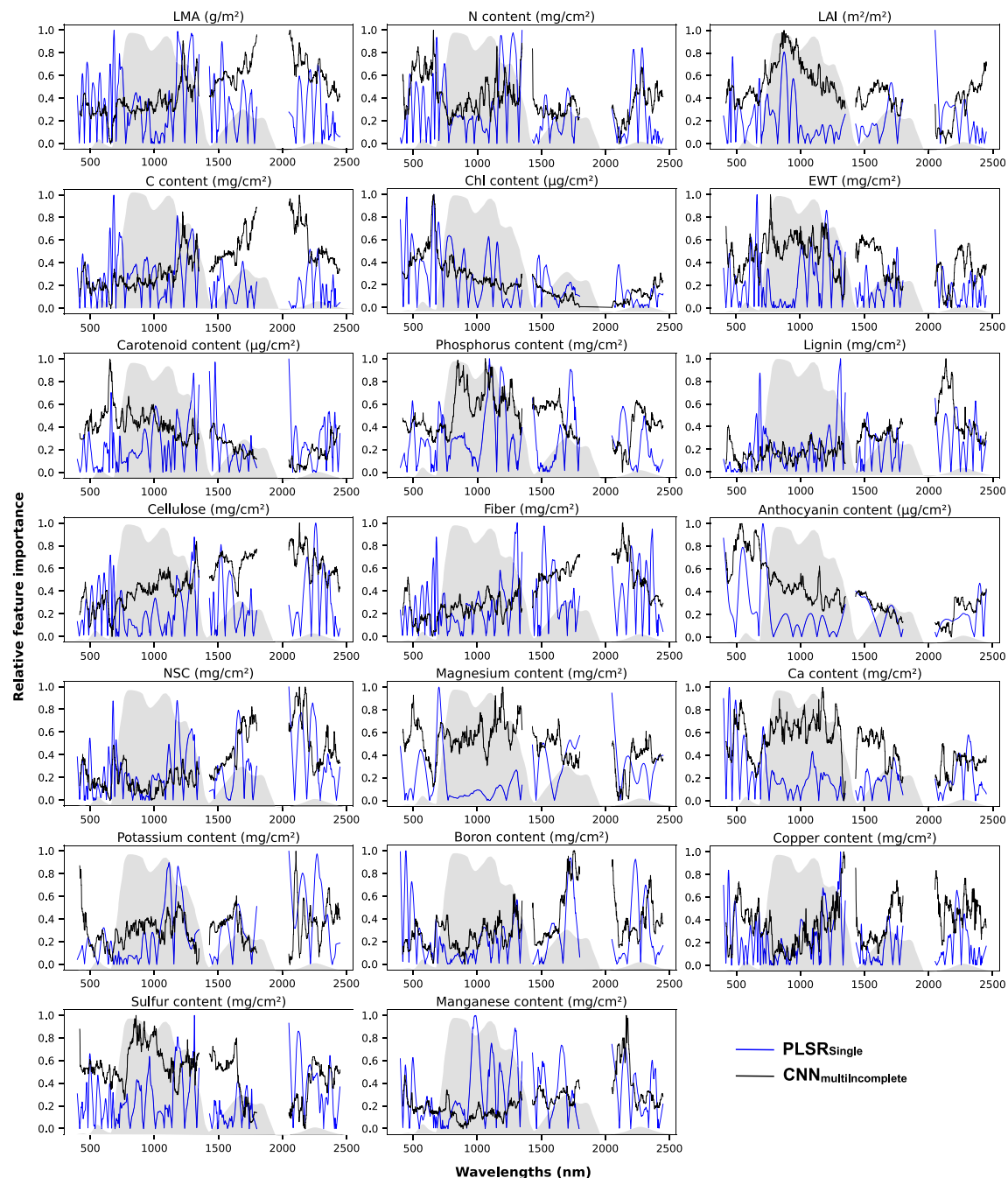


Fig. 8. Relative importance of spectral bands for the prediction of 20 traits using the $\text{CNN}_{\text{multincomplete}}$ and $\text{PLSR}_{\text{single}}$ models. The importance metric of $\text{CNN}_{\text{multincomplete}}$ (Black) is based on the SHAP scores with the gradient explainer, as for $\text{PLSR}_{\text{single}}$ the regression coefficients are shown (Blue). The gray shaded polygon represents a sample vegetation spectrum for orientation. (For interpretation of the references to colour in this figure legend, the reader is referred to the web version of this article.)

broad spectral absorption features and may indirectly facilitate Anth estimation (Jacquemoud and Ustin, 2019; Ollinger, 2011; Ustin et al., 2009). Similarly, nutrients such as Copper, Sulfur, Potassium and Boron do not have distinct spectral absorption features in canopy spectra, but their surprisingly high retrieval performance may be explained by their correlation with other leaf traits that are related to leaf resource investments (Figs. 3, 6) and that have a more explicit spectral response, such as LMA or C (Domínguez et al., 2012; Kothari and Schweiger, 2022).

Largest improvements from single- to multi-trait estimates were found for Lignin, Cellulose and Fiber (Fig. 5), which can be attributed to the high correlation with LMA and C (Fig. 3). Conversely, for LMA, C and

NSC the multi-trait approaches did not result in notable improvements. This may be explained by the fact that these three traits are already very tightly related (chemically and spectrally) and a covariance among these traits does not add further benefit. Moreover, compared to other traits, LMA, C and NSC can be predicted most accurately (Fig. 6), so the covariance with other traits that cannot be predicted as accurately is less likely to facilitate the predictive performance. Similar findings for LMA estimation were found by Furbank et al. (2021) when including the inter-correlation with photosynthetic traits.

We tested three weakly supervised strategies for training the multi-trait models in the context of the data sparsity, i.e. $\text{CNN}_{\text{multincompleteTRY}}$, $\text{CNN}_{\text{multincomplete}}$ and $\text{CNN}_{\text{multinexact}}$. The three strategies

resulted in similar model performance across the traits (e.g. for each strategy, LMA, C and NSC were most accurate and macronutrients least accurate). Yet, CNN_{multiInexact} resulted in the lowest model performance. This is explained by the uncertainty introduced during the spectrally-based gap-filling procedure. However, even with the propagated uncertainty from the gap-filling process, CNN_{multiInexact} outperformed the single-trait models. This demonstrates that such gap-filling strategies are promising to enrich existing sparse data sets, especially as no external knowledge on species or ecosystem type is required. Future attempts may apply a more conservative gap-filling, where data gaps are only filled if the estimated traits are assumed to have a low uncertainty. The uncertainty assessment presented in this study (see Fig. G.1 in Appendix G for details) may be a promising avenue.

The gap-filling strategy based on trait databases (CNN_{multiIncompleteTRY}) significantly improved the performance (compared to CNN_{multiIncomplete}) for those traits that were gap-filled ($p = 0.004$, $w = 82$ Wilcoxon signed-rank test, Table 3, C.3), even when using median trait values by species which do not account for the within-species trait variations. Nonetheless, for the scope of this analysis this does not affect the interpretation of the results as most of the collected samples were taken in the growing season and the results were only evaluated with the original trait obsevations (i.e. no gap-filling). Interestingly, CNN_{multiIncompleteTRY} even improved the model performance for those traits where no gap-filling was performed (due to missing observations in the TRY database, $p = 0.0313$, $w = 15$, Wilcoxon signed-rank test, Fig. 5, Table C.3). This not only underlines the potential of incorporating ancillary trait information, but also highlights the overall value of the multi-trait and corresponding trait-trait relationship. For instance, this has surprisingly influenced the retrieval of Chl and Car, with an improvement of 12–16% in R^2 and 7–7.88% in nRMSE; as well as EWT, Fiber, NSC and Sulfur by 2.00–4.10% in R^2 and 1.68–4.95% in nRMSE. We assume that the growth of trait databases as TRY will even increase the potential of this gap-filling approach.

4.3. Model performance across plant traits

Across all traits, highest model performance was observed for LMA (Fig. 5). This is in line with a series of previous studies highlighting the transferability of models for estimating LMA across data sets at leaf and canopy scale (Serbin et al., 2019; Silva-Perez et al., 2018; Wang et al., 2019, 2020; Helsen et al., 2021; Schiefer et al., 2021; Kothari et al., 2022b). In contrast to these previous studies, the CNN models used here resulted in comparable or even higher model performances although we tested our models using a more diverse data set and exclusively on canopy spectra. The high performance of the LMA estimation is partly a surprise given its broad and overlapping absorption features with water content and scattering components at the canopy scale (Homolová et al., 2013). The high performance of LMA may be partially supported by the ample samples across most of the used data sets (32 data sets out of 42 had LMA observations). Moreover, the robustness of the LMA estimation may also be explained by the overall high correlation of LMA with individual bands across the entire spectrum (Fig. B. 4, Appendix B).

Particularly for LMA but also for most of the other traits, our results suggest that the performances of the multi-trait models are often on par to those of previous studies. For instance, for LAI, Chl, Car and EWT, our models obtained higher performances than Schiefer et al. (2021), who used PLSR models on a data set of canopy spectra across grassland species, which was also integrated in our study. Overall, model performances were comparable to Wang et al. (2020), who used airborne canopy spectra across biomes and to Wang et al. (2019), who used canopy spectra in grasslands. EWT performances were lower than in Wang et al., 2020, where water content was one of the most accurately retrieved traits. The fact that the estimation of EWT was comparably low in the present study may result from the different protocols used across the merged data sets.

In this study we focused on area-based leaf traits due to multiple

reasons: Firstly, as highlighted across different studies in the context of the radiative transfer theory (Dawson et al., 1998; Ganapol et al., 1998; Jacquemoud and Baret, 1990; Vilfan et al., 2016), the retrieval of leaf constituents from spectral signals depends on how much of a leaf constituent (mass) in a given leaf area interacts with light (area-based). In contrast, relative ratios of leaf constituents to LMA (mass-based traits) are not directly related to spectral absorption features (also discussed in Kattenborn et al., 2019b, Zhao et al., 2021). Secondly, normalizing traits on a mass-basis may overshadow the original variation of leaf traits and introduce unrealistic trait-trait-relationships. For instance, photosynthetic traits (e.g. pigments) are generally assumed to be largely independent of leaf resource investments (LMA) (Lloyd et al., 2013; Osnas et al., 2013). This was confirmed for the present data set (Spearman rho <0.4) - but only if the data was scaled on an area-basis (Fig. B.2, Appendix B). As soon as pigments were scaled on a mass-basis, ill-founded correlations were introduced (Spearman rho < -0.73 , see Lloyd et al., 2013 for a statistical rationale). Likewise, traits that directly contribute to the total leaf mass were obviously highly correlated to LMA when compared on an area-basis (spearmans's rho >0.84 for Carbon, NSC, Lignin, Fiber, Cellulose), while a comparably weak relationship was found on a mass-basis (Spearman's rho <0.51). Moreover, we found unrealistically high variation of these LMA-related traits (Carbon, NSC, Lignin, Fiber, Cellulose) when assessed on a mass-basis, which may have mis-lead model calibration (Fig. B.3, Appendix B). Thus, to comply with the physical principles of radiative transfer theory but also reasonable trait-trait relationships, the modeling in the present study was performed exclusively on an area basis.

Note, however, that our proposed models can also be used to derive mass-based traits through normalizing the respective trait prediction by LMA predictions ($\text{trait}_{\text{mass}} = \text{trait}_{\text{area}} / \text{LMA}$). We applied this procedure to compare our model performances to previous studies that performed trait retrieval on a mass-basis (Appendix F). The performances of our baseline multi-trait model (CNN_{multiIncomplete}) with mass-based N and Phosphorus were comparable to studies reviewed in Homolová et al. (2013), while exceeding those of Wang et al. (2020), Asner et al. (2015), Chadwick and Asner (2016), Ewald et al. (2018a) and Wang et al. (2019). The predictive performance for the converted pigments, Fiber, Lignin and Cellulose was lower or comparable to Wang et al. (2020) and Singh et al. (2015) and exceeded those of Asner et al. (2015) and Martin et al. (2018) for tropical forest.

Nevertheless, it should be highlighted that it is often not possible to directly and quantitatively compare model performances across studies, since they frequently differ in vegetation type, modeling approach, model performance metrics and validation strategy, remote sensing platform and sensor, temporal and spatial resolution and extent, simulated and real data, plant traits or a combination of these. Also, the aim and thus the setting of the individual modeling attempts largely differs: some studies aimed to predict traits in a very specific domain and from a very specific platform, while here we aimed to predict traits across different platforms, sensors and vegetation types.

4.4. Model performance across data sets (transferability)

While the 5-fold CV evaluated the model performance with observations that are similar to those observations used in training (internal validation), the model transferability specifically estimated the model performance towards entirely unseen data sets (external validation). The model performances for the transferability evaluation were lower than the internal 5-fold CV (decline of 32% R^2 and 18% nRMSE (mean across traits), Fig. 7, Table E.1 Appendix E). This decline in performance is expected given the large heterogeneity among the data sets (Table 1, Fig. 4) which might largely differ from the training data, e.g. in terms of sensor, platform, illumination conditions, calibration procedure, trait sampling protocol or vegetation type. Overall, in terms of transferability the CNN_{multiIncomplete} model clearly outperformed the PLSR_{single} model (Fig. 7, E.1). This may be explained by the larger number of parameters

in the CNN-based models, which may facilitate learning more abstract spectral features and to resolve spectral features across different sensor or calibration settings. Both CNN- and PLSR-based traits, whose predictions had higher performances with the random internal CV, corresponded to those that had on average the most accurate prediction with the site transferability evaluation. Similar findings have been obtained in [Kothari et al. \(2022\)](#) at the leaf-scale.

Overall, the CNN-based transferability across data sets in this study can be considered as relatively high when compared with previous studies. Even at the leaf-level where spectrally-based trait retrieval is generally less challenging than at the canopy-scale, several studies reported similar or larger drops in performance across traits ([Serbin et al., 2019](#); [Helsen et al., 2021](#); [Kothari et al., 2022b](#)). For instance, the LMA PLSR multi-biome model of [Serbin et al. \(2019\)](#) resulted in R^2 of 0.89 for the internal calibration and dropped to 0.66 when validated externally with LOPEX ([Hosgood et al., 1995](#)) and ANGERS data sets ([Feret et al., 2008](#)) and to 0.68 with the CABO data set (<https://data.caboscience.org/leaf>, [Kothari et al., 2022b,a](#)). [Wang et al. \(2020\)](#) showed a very high model transferability with PLSR models across different vegetation types particularly for LMA and EWT. Likewise, the CNN-based model in [Pullanagari et al. \(2021\)](#) resulted in a robust transferability performance for N retrieval from grasslands where the authors claimed that this can be attributed to the richness of samples from multi-year and multi-site in the training set. However, these studies were based on a consistent sensor and data calibration and processing procedure. This underscores the challenge to train models that are transferable across remote sensing data acquisition settings. However, despite these challenges stemming from the diversity of integrated data sets, the transferability in this study is surprisingly high and we anticipate that with ever increasing data availability more generalized models can be trained in the future.

Eventually, the transferability of models will depend on the feature space distance between the new, unseen data to the training data ([Ludwig et al., 2023](#)). This is confirmed by the model uncertainty estimation procedure developed in this study (Fig. G1 in Appendix G), which is based on this principle and estimates the model uncertainty from the internal CNN embedding, i.e. the feature space viewed from the perspective of the model itself. Such an approach is assumed to be very promising to reveal the area of applicability of a model to new observations and domains ([Meyer and Pebesma, 2021](#)).

4.5. Outlook

As demonstrated in the present study, multi-trait models may not only facilitate high model performances due to the incorporated trait interrelationships, but also provide a tool to simultaneously and, hence, efficiently track multiple traits from remotely sensed hyperspectral data. The multi-trait approach presented here is expandable to more traits and can continuously be improved as new data become available. Instead of retraining the model from scratch, the model weights can be easily updated by retraining the model on new data. In the near future, a large increase in the availability of hyperspectral and trait data can be expected through the availability of operationally scheduled large-scale hyperspectral observations from spaceborne platforms. This goes along with a generally increased incentive for data sharing by the community and institutions and will include future in-situ and airborne campaigns that contribute to the success of global missions such as PRISMA, EnMAP, CHIME and SBG ([Guanter et al., 2015](#); [Labate et al., 2009](#)). Upcoming approaches may also test the integration of simulated data from soil-leaf-canopy RTMs, in the context of hybrid retrieval models (e.g. [Wocher et al., 2022](#); [Verrelst et al., 2021](#)). Such an approach might be particularly promising for traits, vegetation types or states for which only few data are available. In addition, such a physically based approach also takes information about the soil background as well as viewing and observation geometries into account, which may be neglected by empirical approaches.

5. Conclusion

From terrestrial platforms up to satellites, hyperspectral remote sensing is advancing as an important tool for future global monitoring applications. Currently, a significant bottleneck to unleash this potential is the lack of scalable and transferable models. Here, we compiled a large and sparse data set with a wide variability in vegetation types and traits. Our results showed that multi-trait CNN models trained on these data can be more performant than CNN models trained for single traits individually. All tested CNN model approaches outperformed widely-used PLSR models. For multiple traits, the model performances obtained using the CNN multi-trait models were on par to those obtained in previous studies – although the model performances here were estimated from a more diverse data set. This highlights that building robust models requires substantial data variability and only a collaborative effort by the remote sensing community can significantly advance our ability to create models that are transferable across sensors, scales, domains, and ecosystems.

CRediT authorship contribution statement

Eya Cherif: Conceptualization, Methodology, Formal analysis, Data curation, Writing – original draft, Visualization. **Hannes Feilhauer:** Data curation, Conceptualization, Writing – original draft, Supervision. **Katja Berger:** Data curation, Writing – review & editing. **Phuong D. Dao:** Data curation, Writing – review & editing. **Michael Ewald:** Data curation, Writing – review & editing. **Tobias B. Hank:** Data curation, Writing – review & editing. **Yuhong He:** Data curation, Writing – review & editing. **Kyle R. Kovach:** Data curation, Writing – review & editing. **Bing Lu:** Data curation, Writing – review & editing. **Philip A. Townsend:** Data curation, Writing – review & editing. **Teja Kattenborn:** Data curation, Conceptualization, Writing – original draft, Supervision.

Declaration of Competing Interest

The authors declare that they have no known competing financial interests or personal relationships.

Data availability

The code, the data and trained model objects are available on Gitlab: <https://gitlab.com/eya95/multi-traitretrieval>.

Acknowledgements

We thank all data owners for sharing the data either by request (in particular the consortium of the EU BiodivERsA project DIARS) or through the public Ecological Spectral Information System (EcoSIS), Data Publisher for Earth & Environmental Science (PANGEA) and DRYAD platforms. The authors acknowledge the financial support by the Federal Ministry of Education and Research of Germany (BMBF) and by the Sächsische Staatsministerium für Wissenschaft Kultur und Tourismus in the program Center of Excellence for AI-research “Center for Scalable Data Analytics and Artificial Intelligence Dresden/Leipzig”, project identification number: ScaDS.AI. Further support of this work was granted by the Federal Ministry for Economic Affairs and Climate Action (BMWK) and the German Aerospace Center (DLR) through the project AIResVeg (grant 50EE2203A) and the EnMAP scientific preparation program (grants 50EE0947, 50EE1308 and 50EE1623). Support for Dao, Kovach and Townsend was provided by US National Science Foundation (NSF), Macrosystems Biology and NEON-Enabled Science grant DEB-1638720 and NSF Biology Integration Institute award DBI-2021898.

Appendix A. Supplementary data

Supplementary data to this article can be found online at <https://doi.org/10.1016/j.rse.2023.113580>.

References

- Ainsworth, E.A., Serbin, S.P., Skoneczka, J.A., Townsend, P.A., 2014. Using leaf optical properties to detect ozone effects on foliar biochemistry. *Photosynth. Res.* 119, 65–76.
- Asner, G.P., Martin, R.E., 2016. Spectromics: emerging science and conservation opportunities at the interface of biodiversity and remote sensing. *Glob. Ecol. Conserv.* 8, 212–219.
- Asner, G.P., Martin, R.E., 2008. Spectral and chemical analysis of tropical forests: scaling from leaf to canopy levels. *Remote Sens. Environ.* 112, 3958–3970.
- Asner, G.P., Martin, R.E., Anderson, C.B., Knapp, D.E., 2015. Quantifying forest canopy traits: imaging spectroscopy versus field survey. *Remote Sens. Environ.* 158, 15–27.
- Atzberger, C., Richter, K., 2012. Spatially constrained inversion of radiative transfer models for improved LAI mapping from future Sentinel-2 imagery. *Remote Sens. Environ.* 120, 208–218.
- Berger, K., Machowitz, M., Kycko, M., Kefauver, S.C., van Wittenbergh, S., et al., 2022. Multi-sensor spectral synergies for crop stress detection and monitoring in the optical domain: a review. *Remote Sens. Environ.* 280, 113198.
- Berger, K., Verrelst, J., Feret, J.-B., Wang, Z., Woher, M., Strathmann, M., Danner, M., Mauser, W., Hank, T., 2020. Crop nitrogen monitoring: recent progress and principal developments in the context of imaging spectroscopy missions. *Remote Sens. Environ.* 242, 111758.
- Berger, K., Atzberger, C., Danner, M., D'Urso, G., Mauser, W., et al., 2018. Evaluation of the PROSAIL model capabilities for future hyperspectral model environments: a review study. *Remote Sens.* 10, 85.
- Billings, W.D., Morris, R.J., 1951. Reflection of visible and infrared radiation from leaves of different ecological groups. *Am. J. Bot.* 327–331.
- Burnett, A.C., Serbin, S.P., Rogers, A., 2021. Source: sink imbalance detected with leaf- and canopy-level spectroscopy in a field-grown crop. *Plant Cell Environ.* 44, 2466–2479.
- Cavender-Bares, J., Gamon, J.A., Townsend, P.A., 2020. The use of remote sensing to enhance biodiversity monitoring and detection: A critical challenge for the twenty-first century. In: *Remote Sensing of Plant Biodiversity*. Springer, Cham, pp. 1–12.
- Cawse-Nicholson, K., Townsend, P.A., Schimel, D., Assiri, A.M., Blake, P.L., et al., 2021. NASA's surface biology and geology designated observable: a perspective on surface imaging algorithms. *Remote Sens. Environ.* 257, 112349.
- Cerasoli, S., Campagnolo, M., Faria, J., Nogueira, C., da Caldeira, M., C., 2018. On estimating the gross primary productivity of Mediterranean grasslands under different fertilization regimes using vegetation indices and hyperspectral reflectance. *Biogeosciences* 15, 5455–5471.
- Chadwick, K.D., Asner, G.P., 2016. Organismic-scale remote sensing of canopy foliar traits in lowland tropical forests. *Remote Sens.* 8, 87.
- Chen, S., Hong, X., Harris, C.J., Sharkey, P.M., 2004. Sparse modeling using orthogonal forward regression with PRESS statistic and regularization. *IEEE Trans. Syst. Man Cybernet. Part B* 34, 898–911.
- Chlus, A., Kruger, E.L., Townsend, P.A., 2020. Mapping three-dimensional variation in leaf mass per area with imaging spectroscopy and lidar in a temperate broadleaf forest. *Remote Sens. Environ.* 250, 112043.
- Cogliati, S., Sarti, F., Chiarantini, L., Cosi, M., Lorusso, R., et al., 2021. The PRISMA imaging spectroscopy mission: overview and first performance analysis. *Remote Sens. Environ.* 262, 112499.
- Cui, C., Fearn, T., 2018. Modern practical convolutional neural networks for multivariate regression: applications to NIR calibration. *Chemom. Intell. Lab. Syst.* 182, 9–20.
- Damerau, F.J., 1964. A technique for computer detection and correction of spelling errors. *Commun. ACM* 7, 171–176.
- Danner, M., Berger, K., Woher, M., Mauser, W., Hank, T., 2021. Efficient RTM-based training of machine learning regression algorithms to quantify biophysical & biochemical traits of agricultural crops. *ISPRS J. Photogramm. Remote Sens.* 173, 278–296.
- Dao, P.D., Axiotis, A., He, Y., 2021. Mapping native and invasive grassland species and characterizing topography-driven species dynamics using high spatial resolution hyperspectral imagery. *Int. J. Appl. Earth Obs. Geoinf.* 104, 102542 <https://doi.org/10.1016/j.jag.2021.102542>.
- Dawson, T.P., Curran, P.J., Plummer, S.E., 1998. LIBERTY—Modeling the effects of leaf biochemical concentration on reflectance spectra. *Remote Sens. Environ.* 65, 50–60.
- de Bello, F., Lavorel, S., Diaz, S., Harrington, R., Cornelissen, J.H.C., et al., 2010. Towards an assessment of multiple ecosystem processes and services via functional traits. *Biodivers. Conserv.* 19, 2873–2893.
- Díaz, S., Kattge, J., Cornelissen, J.H.C., Wright, I.J., Lavorel, S., et al., 2016. The global spectrum of plant form and function. *Nature* 529, 167–171.
- Dominguez, M.T., Aponte, C., Pérez-Ramos, I.M., García, L.V., Villar, R., Marañón, T., 2012. Relationships between leaf morphological traits, nutrient concentrations and isotopic signatures for Mediterranean woody plant species and communities. *Plant Soil* 357, 407–424.
- Dorigo, W.A., Zurita-Milla, R., de Wit, A.J.W., Brazile, J., Singh, R., Schaepman, M.E., 2007. A review on reflective remote sensing and data assimilation techniques for enhanced agroecosystem modeling. *Int. J. Appl. Earth Obs. Geoinf.* 9, 165–193.
- Ewald, M., Aerts, R., Lenoir, J., Fassnacht, F.E., Nicolas, M., et al., 2018a. LiDAR derived forest structure data improves predictions of canopy N and P concentrations from imaging spectroscopy. *Remote Sens. Environ.* 211, 13–25.
- Ewald, M., Skowronek, S., Aerts, R., Dolos, K., Lenoir, J., et al., 2018b. Analyzing remotely sensed structural and chemical canopy traits of a forest invaded by *Prunus serotina* over multiple spatial scales. *Biol. Invasions* 20, 2257–2271.
- Ewald, M., Skowronek, S., Aerts, R., Lenoir, J., Feilhauer, H., et al., 2020. Assessing the impact of an invasive bryophyte on plant species richness using high resolution imaging spectroscopy. *Ecol. Indic.* 110, 105882.
- Feilhauer, H., Schmid, T., Faude, U., Sanchez-Carrillo, S., Cirujano, S., 2018. Are remotely sensed traits suitable for ecological analysis? A case study of long-term drought effects on leaf mass per area of wetland vegetation. *Ecol. Indic.* 88, 232–240.
- Feilhauer, H., Somers, B., van der Linden, S., 2017. Optical trait indicators for remote sensing of plant species composition: predictive power and seasonal variability. *Ecol. Indic.* 73, 825–833.
- Feilhauer, H., Asner, G.P., Martin, R.E., Schmidlein, S., 2010. Brightness-normalized partial least squares regression for hyperspectral data. *J. Quant. Spectrosc. Radiat. Transf.* 111, 1947–1957.
- Féret, J.-B., Berger, K., de Boissieu, F., Malenovsky, Z., 2021. PROSPECT-PRO for estimating content of nitrogen-containing leaf proteins and other carbon-based constituents. *Remote Sens. Environ.* 252, 112173.
- Féret, J.-B., Gitelson, A.A., Noble, S.D., Jacquemoud, S., 2017. PROSPECT-D: towards modeling leaf optical properties through a complete lifecycle. *Remote Sens. Environ.* 193, 204–215.
- Féret, J.-B., François, C., Asner, G.P., Gitelson, A.A., Martin, R.E., et al., 2008. PROSPECT-4 and 5: advances in the leaf optical properties model separating photosynthetic pigments. *Remote Sens. Environ.* 112, 3030–3043.
- Funk, J.L., Larson, J.E., Ames, G.M., Butterfield, B.J., Cavender-Bares, J., et al., 2017. Revisiting the holy grail: using plant functional traits to understand ecological processes. *Biol. Rev.* 92, 1156–1173.
- Furbank, R.T., Silva-Perez, V., Evans, J.R., Condon, A.G., Estavillo, G.M., et al., 2021. Wheat physiology predictor: predicting physiological traits in wheat from hyperspectral reflectance measurements using deep learning. *Plant Methods* 17, 1–15.
- Gates, D.M., Keegan, H.J., Schleter, J.C., Weidner, V.R., 1965. Spectral properties of plants. *Appl. Opt.* 4, 11–20.
- Ganapol, B.D., Johnson, L.F., Hammer, P.D., Hlavka, C.A., Peterson, D.L., 1998. LEAFMOD: a new within-leaf radiative transfer model. *Remote Sens. Environ.* 63, 182–193.
- Geladi, P., Kowalski, B.R., 1986. Partial least-squares regression: a tutorial. *Anal. Chim. Acta* 185, 1–17.
- Goodfellow, I., Bengio, Y., Courville, A., 2016. Deep learning. MIT press.
- Grime, J.P., 1988. The CSR model of primary plant strategies—origins, implications and tests. In: *Plant Evolutionary Biology*. Springer, pp. 371–393.
- Guanter, L., Kaufmann, H., Segl, K., Foerster, S., Rogass, C., et al., 2015. The EnMAP spaceborne imaging spectroscopy mission for earth observation. *Remote Sens.* 7, 8830–8857.
- Hank, T.B., Berger, K., Bach, H., Clevers, J.G.P.W., Gitelson, A., et al., 2019. Spaceborne imaging spectroscopy for sustainable agriculture: contributions and challenges. *Surv. Geophys.* 40, 515–551.
- Hank, T., Locherer, M., Richter, K., Mauser, W., Consortium, E., 2016. Neusling (Landau ad Isar) 2012-a multitemporal and multisensor agricultural EnMAP Preparatory Flight Campaign.
- Hank, T., Richter, K., Mauser, W., Consortium, E., 2015. Neusling (Landau ad Isar) 2009—an agricultural EnMAP Preparatory Flight Campaign using the HyMap instrument.
- Heckmann, D., Schlüter, U., Weber, A.P.M., 2017. Machine learning techniques for predicting crop photosynthetic capacity from leaf reflectance spectra. *Mol. Plant* 10, 878–890.
- Heckmann, David, Urte Schlüter, Andreas, PM Weber, 2017. Machine learning techniques for predicting crop photosynthetic capacity from leaf reflectance spectra. *Mol. plant* 10 (6), 878–890.
- Helsen, K., Bassi, L., Feilhauer, H., Kattenborn, T., Matsushima, H., et al., 2021. Evaluating different methods for retrieving intraspecific leaf trait variation from hyperspectral leaf reflectance. *Ecol. Indic.* 130, 108111.
- Herrmann, I., Pimstein, A., Karnieli, A., Cohen, Y., Alchanatis, V., Bonfil, D.J., 2011. LAI assessment of wheat and potato crops by VENµS and Sentinel-2 bands. *Remote Sens. Environ.* 115, 2141–2151.
- Hill, J., Buddenbaum, H., Townsend, P.A., 2019. Imaging spectroscopy of forest ecosystems: perspectives for the use of space-borne hyperspectral earth observation systems. *Surv. Geophys.* 40, 553–588.
- Hinton, G.E., Srivastava, N., Krizhevsky, A., Sutskever, I., Salakhutdinov, R.R., 2012. Improving neural networks by preventing co-adaptation of feature detectors *arXiv preprint arXiv:1207.0580*.
- Homolová, L., Malenovsky, Z., Clevers, J.G.P.W., Garcia-Santos, G., Schaepman, M.E., 2013. Review of optical-based remote sensing for plant trait mapping. *Ecol. Complex.* 15, 1–16.
- Hosgood, B., Jacquemoud, S., Andreoli, G., Verdebout, J., Pedrini, G., Schmuck, G., 1995. Leaf optical properties experiment 93 (LOPEX93). Report EUR 16095.
- Jacquemoud, S., Baret, F., 1990. PROSPECT: a model of leaf optical properties spectra. *Remote Sens. Environ.* 34, 75–91.
- Jacquemoud, S., Verhoef, W., Baret, F., Bacour, C., Zarco-Tejada, P., et al., 2009. Use of prospect+ sail to estimate canopy biochemistry at different scales. *Remote Sens. Environ.* 113, S56–S66.
- Jacquemoud, S., Ustin, S., 2019. Leaf optical properties. Cambridge University Press.

- Janet, J.P., Duan, C., Yang, T., Nandy, A., Kulik, H.J., 2019. A quantitative uncertainty metric controls error in neural network-driven chemical discovery. *Chem. Sci.* 10, 7913–7922.
- Jetz, W., Cavender-Bares, J., Pavlick, R., Schimel, D., Davis, F.W., Asner, G.P., et al., 2016. Monitoring plant functional diversity from space. *Nat. Plants* 2, 1–5.
- Kattenborn, T., Schiefer, F., Frey, J., Feilhauer, H., Mahecha, M.D., Dormann, C.F., 2022. Spatially autocorrelated training and validation samples inflate performance assessment of convolutional neural networks. *ISPRS Open J. Photogramm. Remote Sens.* 5, 100018.
- Kattenborn, T., Leitloff, J., Schiefer, F., Hinz, S., 2021. Review on convolutional neural networks (CNN) in vegetation remote sensing. *ISPRS J. Photogramm. Remote Sens.* 173, 24–49.
- Kattenborn, T., Schiefer, F., Zarco-Tejada, P., Schmidlein, S., 2019b. Advantages of retrieving pigment content [$\mu\text{g}/\text{cm}^2$] versus concentration [%] from canopy reflectance. *Remote Sens. Environ.* 230, 111195.
- Kattenborn, T., Fasnacht, F.E., Schmidlein, S., 2019a. Differentiating plant functional types using reflectance: which traits make the difference? *Remote Sens. Ecol. Conserv.* 5, 5–19.
- Kattenborn, T., Schmidlein, S., 2019. Radiative transfer modelling reveals why canopy reflectance follows function. *Sci. Rep.* 9, 1–10.
- Kattge, J., Bönnisch, G., Díaz, S., Lavorel, S., Prentice, I.C., et al., 2020. TRY plant trait database - enhanced coverage and open access. *Glob. Chang. Biol.* 26, 119–188. <https://doi.org/10.1111/gcb.14904>.
- Kingma, D.P., Ba, J., 2014. Adam: A method for stochastic optimization arXiv preprint arXiv:1412.6980.
- Kokaly, R.F., Asner, G.P., Ollinger, S.V., Martin, M.E., Wessman, C.A., 2009. Characterizing canopy biochemistry from imaging spectroscopy and its application to ecosystem studies. *Remote Sens. Environ.* 113, S78–S91.
- Konstantinidis, S., 2005. Computing the Levenshtein distance of a regular language. In: IEEE Information Theory Workshop, 2005, p. 4.
- Kothari, S., Beauchamp-Rioux, R., Blanchard, F., Crofts, L., Girard, A., Guilbeault-Mayers, X., Hacker, W., Pardo, J., Schweiger, K., Demers-Thibeault, S., Bruneau, A., Coops, C., Kalacska, M., Vellend, M., Lalibert, E., 2022a. CABO 2018–2019 Leaf-Level Spectra.
- Kothari, S., Schweiger, A.K., 2022. Plant spectra as integrative measures of plant phenotypes. *J. Ecol.* 110, 2536–2554.
- Kothari, S., Beauchamp-Rioux, R., Blanchard, F., Crofts, A.L., Girard, A., Guilbeault-Mayers, X., Hacker, P.W., Pardo, J., Schweiger, A.K., Demers-Thibeault, S., 2022b. Predicting leaf traits across functional groups using reflectance spectroscopy bioRxiv 2022–2027.
- Labate, D., Ceccherini, M., Cisbani, A., de Cosmo, V., Galeazzi, 2009. The PRISMA payload optomechanical design, a high performance instrument for a new hyperspectral mission. *Acta Astronaut.* 65, 1429–1436.
- Lavorel, S., Garnier, É., 2002. Predicting changes in community composition and ecosystem functioning from plant traits: revisiting the holy grail. *Funct. Ecol.* 16, 545–556.
- Lichtenthaler, H.K., 1987. [34] chlorophylls and carotenoids: pigments of photosynthetic biomembranes. *Methods Enzymol.* Elsevier 350–382.
- Lloyd, J., Bloomfield, K., Domingues, T.F., Farquhar, G.D., 2013. Photosynthetically relevant foliar traits correlating better on a mass vs an area basis: of ecophysiological relevance or just a case of mathematical imperatives and statistical quicksand? *New Phytol.* 199, 311–321.
- Ludwig, M., Moreno-Martinez, A., Hözel, N., Pebesma, E., Meyer, H., 2023. Assessing and improving the transferability of current global spatial prediction models. *Glob. Ecol. and Biogeography.* 32, 356–368.
- Lundberg, S.M., Lee, S.-I., 2017. A unified approach to interpreting model predictions. *Adv. Neural Inf. Process. Syst.* 30.
- Martin, R.E., Chadwick, K.D., Brodrick, P.G., Carranza-Jimenez, L., Vaughn, N.R., Asner, G.P., 2018. An approach for foliar trait retrieval from airborne imaging spectroscopy of tropical forests. *Remote Sens.* 10 (2), 199.
- Meyer, H., Pebesma, E., 2021. Predicting into unknown space? Estimating the area of applicability of spatial prediction models. *Methods Ecol. Evol.* 12, 1620–1633.
- Migliavacca, M., Musavi, T., Mahecha, M.D., Nelson, J.A., Knauer, J., Baldocchi, D.D., Perez-Priego, O., Christansen, R., Peters, J., Anderson, K., et al., 2021. The three major axes of terrestrial ecosystem function. *Nature* 598, 468–472.
- Mila, C., Mateu, J., Pebesma, E., Meyer, H., 2022. Nearest neighbour distance matching leave-one-out cross-validation for map validation. *Methods Ecol. Evol.* 13, 1304–1316.
- Ng, W., Minasny, B., Montazerolghaem, M., Padarian, J., Ferguson, R., Bailey, S., McBratney, A.B., 2019. Convolutional neural network for simultaneous prediction of several soil properties using visible/near-infrared, mid-infrared, and their combined spectra. *Geoderma* 352, 251–267.
- Ollinger, S.V., 2011. Sources of variability in canopy reflectance and the convergent properties of plants. *New Phytol.* 189, 375–394.
- Osnas, J.L.D., Lichstein, J.W., Reich, P.B., Pacala, S.W., 2013. Global leaf trait relationships: mass, area, and the leaf economics spectrum. *Science* 340 (741–744).
- Padarian, J., Minasny, B., McBratney, A.B., 2019. Using deep learning to predict soil properties from regional spectral data. *Geoderma Reg.* 16, e00198.
- Poorter, H., Niinemets, Ü., Poorter, L., Wright, I.J., Villar, R., 2009. Causes and consequences of variation in leaf mass per area (LMA): a meta-analysis. *New Phytol.* 182, 565–588.
- Pottier, J., Malenovsky, Z., Psomas, A., Homolová, L., Schaepman, M.E., et al., 2014. Modelling plant species distribution in alpine grasslands using airborne imaging spectroscopy. *Biol. Lett.* 10, 20140347.
- Prilianti, K.R., Setiyono, E., Kelana, O.H., Brotosudarmo, T.H.P., 2021. Deep chemometrics for nondestructive photosynthetic pigments prediction using leaf reflectance spectra. *Inform. Process. Agric.* 8, 194–204.
- Pullanagari, R.R., Dehghan-Shoar, M., Yule, I.J., Bhatia, N., 2021. Field spectroscopy of canopy nitrogen concentration in temperate grasslands using a convolutional neural network. *Remote Sens. Environ.* 257, 112353.
- Ramsundar, B., Kearnes, S., Riley, P., Webster, D., Konerding, D., Pande, V., 2015. Massively multitask networks for drug discovery arXiv preprint arXiv:1502.02072.
- Rogers, A., Serbin, S., Ely, K., 2021. Leaf Mass Area, Leaf Carbon and Nitrogen Content, Kougarok Road and Teller Road, Seward Peninsula, Alaska.
- Savitzky, A., Golay, M.J.E., 1964. Smoothing and differentiation of data by simplified least squares procedures. *Anal. Chem.* 36, 1627–1639.
- Schiefer, F., Schmidlein, S., Kattenborn, T., 2021. The retrieval of plant functional traits from canopy spectra through RTM-inversions and statistical models are both critically affected by plant phenology. *Ecol. Indic.* 121, 107062.
- Schrodt, F., Kattge, J., Shan, H., Fazayeli, F., Joswig, J., et al., 2015. BHPMF—a hierarchical Bayesian approach to gap-filling and trait prediction for macroecology and functional biogeography. *Glob. Ecol. Biogeogr.* 24, 1510–1521.
- Serbin, S.P., Wu, J., Ely, K.S., Kruger, E.L., Townsend, P.A., et al., 2019. From the Arctic to the tropics: multibiomass prediction of leaf mass per area using leaf reflectance. *New Phytol.* 224, 1557–1568.
- Shan, H., Kattge, J., Reich, P., Banerjee, A., Schrodt, F., Reichstein, M., 2012. Gap Filling in the Plant Kingdom—Trait Prediction Using Hierarchical Probabilistic Matrix Factorization arXiv preprint arXiv:1206.6439.
- Shi, S., Xu, L., Gong, W., Chen, Bowen, et al., 2022. A convolution neural network for forest leaf chlorophyll and carotenoid estimation using hyperspectral reflectance. *Int. J. Appl. Earth Obs. Geoinf.* 108, 102719.
- Shin, H.-C., Roth, H.R., Gao, M., Lu, L., Xu, Z., Nogues, I., Yao, J., Mollura, D., Summers, R.M., 2016. Deep convolutional neural networks for computer-aided detection: CNN architectures, dataset characteristics and transfer learning. *IEEE Trans. Med. Imaging* 35, 1285–1298.
- Silva-Perez, V., Molero, G., Serbin, S.P., Condon, A.G., Reynolds, M.P., et al., 2018. Hyperspectral reflectance as a tool to measure biochemical and physiological traits in wheat. *J. Exp. Bot.* 69, 483–496.
- Singh, A., Serbin, S.P., McNeil, B.E., Kingdon, C.C., Townsend, P.A., 2015. Imaging spectroscopy algorithms for mapping canopy foliar chemical and morphological traits and their uncertainties. *Ecol. Appl.* 25, 2180–2197.
- Smilkov, D., Thorat, N., Kim, B., Viégas, F., Wattenberg, M., 2017. Smoothgrad: removing noise by adding noise arXiv preprint arXiv:1706.03825.
- Sosnin, S., Vashurina, M., Withnall, M., Karpov, P., Fedorov, M., Tetko, I.V., 2019. A survey of multi-task learning methods in chemoinformatics. *Mol. Inform.* 38, 1800108.
- Sundararajan, M., Taly, A., Yan, Q., 2017. Axiomatic attribution for deep networks, international conference on. *Mach. Learn.* 3319–3328.
- Tan, M., Le, Q., 2019. Efficientnet: rethinking model scaling for convolutional neural networks. *Int. Conf. Mach. Learn.* 6105–6114.
- Tsakiridis, N.L., Keramaris, K.D., Theocaris, J.B., Zalidis, G.C., 2020. Simultaneous prediction of soil properties from VNIR-SWIR spectra using a localized multi-channel 1D convolutional neural network. *Geoderma* 367, 114208.
- Ustin, S.L., Gamon, J.A., 2010. Remote sensing of plant functional types. *New Phytol.* 186, 795–816.
- Ustin, S.L., Gitelson, A.A., Jacquemoud, S., Schaepman, M., Asner, G.P., 2009. Retrieval of foliar information about plant pigment systems from high resolution spectroscopy. *Remote Sens. Environ.* 113, S67–S77.
- van Cleemput, E., Roberts, D.A., Honnay, O., Somers, B., 2019. A novel procedure for measuring functional traits of herbaceous species through field spectroscopy. *Methods Ecol. Evol.* 10, 1332–1338.
- van Cleemput, E., Vanierschot, L., Fernández-Castilla, B., Honnay, O., Somers, B., 2018. The functional characterization of grass- and shrubland ecosystems using hyperspectral remote sensing: trends, accuracy and moderating variables. *Remote Sens. Environ.* 209, 747–763.
- Verrelst, J., Rivera-Caicedo, J.P., Reyes-Muñoz, P., Morata, M., Amin, E., et al., 2021. Mapping landscape canopy nitrogen content from space using PRISMA data. *ISPRS J. Photogramm. Remote Sens.* 178, 382–395.
- Verrelst, J., Malenovsky, Z., der Tol, C., Camps-Valls, G., Gastellu-Etchegorry, J.-P., et al., 2019. Quantifying vegetation biophysical variables from imaging spectroscopy data: a review on retrieval methods. *Surv. Geophys.* 40, 589–629.
- Verrelst, J., Rivera, J.P., Leonenko, G., Alonso, L., Moreno, J., 2013. Optimizing LUT-based RTM inversion for semiautomatic mapping of crop biophysical parameters from Sentinel-2 and -3 data: role of cost functions. *IEEE Trans. Geosci. Remote Sens.* 52, 257–269.
- Vilfan, N., der Tol, C., Müller, O., Rascher, U., Verhoef, W., 2016. Fluspect-B: a model for leaf fluorescence, reflectance and transmittance spectra. *Remote Sens. Environ.* 186, 596–615.
- Wagner, E.P., Merz, J., Townsend, P.A., 2018. Ecological spectral information system: an open spectral library. *AGU Fall Meet. Abst.* B41L-B2878L.
- Wang, Z., Chlus, A., Geygan, R., Ye, Z., Zheng, T., et al., 2020. Foliar functional traits from imaging spectroscopy across biomes in eastern North America. *New Phytol.* 228, 494–511.
- Wang, Z., Townsend, P.A., Schweiger, A.K., Couture, J.J., Singh, A., et al., 2019. Mapping foliar functional traits and their uncertainties across three years in a grassland experiment. *Remote Sens. Environ.* 221, 405–416.
- Wocher, M., Berger, K., Verrelst, J., Hank, T., 2022. Retrieval of carbon content and biomass from hyperspectral imagery over cultivated areas. *ISPRS J. Photogramm. Remote Sens.* 193, 104–114.

- Wocher, M., Berger, K., Danner, M., Mauser, W., Hank, T., 2018. Physically-based retrieval of canopy equivalent water thickness using hyperspectral data. *Remote Sens.* 10, 1924.
- Wold, S., Ruhe, A., Wold, H., Dunn Iii, W.J., 1984. The collinearity problem in linear regression. The partial least squares (PLS) approach to generalized inverses. *SIAM J. Sci. Stat. Comput.* 5, 735–743.
- Wold, S., Sjöström, M., Eriksson, L., 2001. PLS-regression: a basic tool of chemometrics. *Chemom. Intell. Lab. Syst.* 58, 109–130.
- Yang, Y., Zhu, Q., Peng, C., Wang, H., Chen, H., 2015. From plant functional types to plant functional traits: a new paradigm in modelling global vegetation dynamics. *Prog. Phys. Geogr.* 39, 514–535.
- Yosinski, J., Clune, J., Bengio, Y., Lipson, H., 2014. How transferable are features in deep neural networks? *Adv. Neural Inf. Process. Syst.* 27.
- Zarco-Tejada, P.J., Camino, C., Beck, P.S.A., Calderon, R., Hornero, A., et al., 2018. Previsual symptoms of *Xylella fastidiosa* infection revealed in spectral plant-trait alterations. *Nat. Plants* 4, 432–439.
- Zarco-Tejada, P.J., Hornero, A., Beck, P.S.A., Kattenborn, T., Kempeneers, P., Hernández-Clemente, R., 2019. Chlorophyll content estimation in an open-canopy conifer forest with sentinel-2A and hyperspectral imagery in the context of forest decline. *Remote Sens. Environ.* 223, 320–335.
- Zhang, Y., Yang, Q., 2021. A survey on multi-task learning. *IEEE Trans. Knowl. Data Eng.* 34, 5586–5609.
- Zhao, Y., Sun, Y., Lu, X., Zhao, X., Yang, L., Sun, Z., Bai, Y., 2021. Hyperspectral retrieval of leaf physiological traits and their links to ecosystem productivity in grassland monocultures. *Ecol. Indic.* 122, 107267.
- Zhou, Zhi-Hua., 2018. A brief introduction to weakly supervised learning. *Natl. Sci. Rev.* 5 (1), 44–53.
- Zhu, X.X., Tuia, D., Mou, L., Xia, G.-S., Zhang, L., Xu, F., Fraundorfer, F., 2017. Deep learning in remote sensing: a comprehensive review and list of resources. *IEEE Geosci. Remote Sens. Mag.* 5, 8–36.